PART 1

Fundamental concepts of atrial fibrillation

1

CHAPTER 1

Anatomy of the left atrium relevant to atrial fibrillation ablation

José Angel Cabrera, Jerónimo Farré, Siew Yen Ho, & Damián Sánchez-Quintana

Introduction

Atrial fibrillation (AF) is an arrhythmia most likely due to multiple etiopathogenic mechanisms. In spite of a still incomplete understanding of the anatomo-functional basis for the initiation and maintenance of AF, various radiofrequency catheter ablation (RFCA) techniques have been shown to modify the substrate of the arrhythmia and/or its neurovegetative modulators, achieving in a high proportion of cases a sustained restoration of a stable sinus rhythm [1–26]. Catheter ablation techniques in patients with AF have evolved from an initial approach focused on the pulmonary veins (PVs) and their junctions with the left atrium (LA), to a more extensive intervention mainly, but not exclusively, on the left atrial myocardium and its neurovegetative innervation [27–32]. We firmly believe that progress is still required to refine the currently accepted catheter ablation approaches to AF. Because the LA is the main target of catheter ablation in patients with AF, in this chapter we review the gross morphological and architectural features of this chamber and its relations with extracardiac structures. The latter have also become relevant because of some extracardiac complications of AF ablation, such as injuries of the phrenic and vagal plexus nerves, or the devastating left atrioesophageal fistula formation [33–40].

Components of the left atrium

From a gross anatomical viewpoint the LA has four components: (1) a venous part that receives the PVs; (2) a vestibule that conducts to the mitral valve; (3) the left atrial appendage (LAA); and (4) the so-called interatrial septum. We want to emphasize that the true interatrial septum is the oval fossa, a depression in the right atrial aspect of the area traditionally considered to be the interatrial septum [41–46] (Figures 1.1–1.4). At the left atrial level, a membranous valve covers this region and conceptually represents the only true interatrial septum in the sense that it can be crossed without exiting the heart. The rest of the "muscular interatrial septum" is formed by the apposition of the right and left atrial myocardia that are separated by vascularized fibro-fatty tissues extending from the extracardiac fat. This is why we prefer to use the term *interatrial groove* rather than muscular interatrial septum, a concept that is not only of academic interest because trans-septal punctures to access the LA should be performed through the oval fossa (Figure 1.2). Thus, a puncture throughout the interatrial groove (the muscular interatrial septum)

Catheter Ablation of Atrial Fibrillation Edited by Etienne Aliot, Michel Haïssaguerre and Warren M. Jackman
 ISBN: 978-1-4501-6349-1.

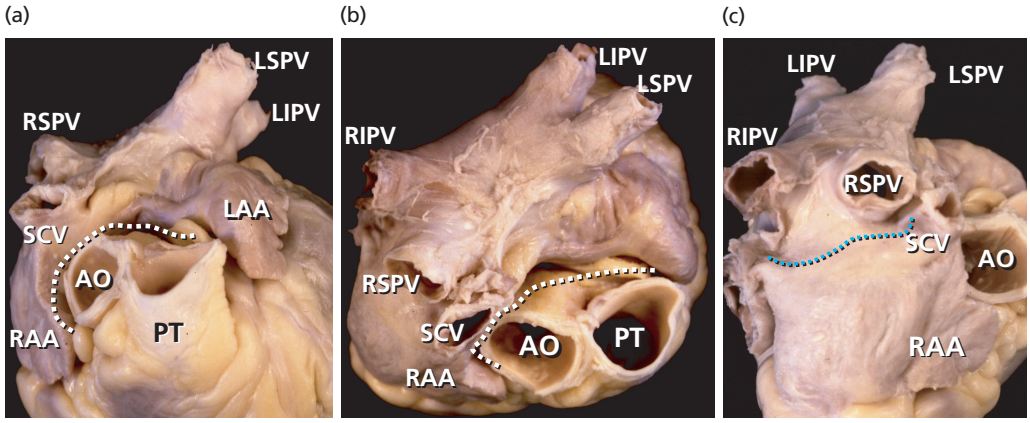

Figure 1.1 External appearances of the right and left atriums viewed from anterior (a), superior (b), and right lateral (c) views. Note the location of the transverse sinus (white dotted lines) and its relationship to the aorta and atrial walls (a, b). The superior and posterior walls of the LA were anchored by the entrance of one PV at each of the four corners. (c) Site of the interatrial groove (Waterston's groove, blue dotted line). AO, aorta; LAA, left atrial appendage; LIPV, left inferior pulmonary vein; LSPV, left superior PV; PT, pulmonary trunk; RAA, right atrial appendage; RIPV, right inferior pulmonary vein; RSPV, right superior pulmonary vein; SCV, superior caval vein.

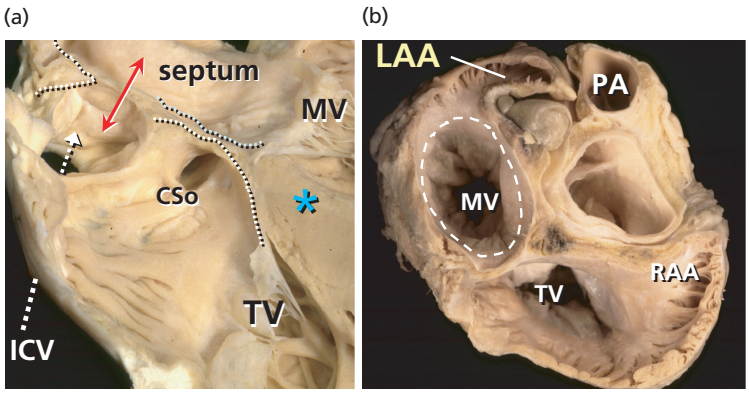

Figure 1.2 (a) Four-chamber section through the heart showing the offset arrangement of the mitral valve (MV) and tricuspid valve (TV) which produces the so-called muscular atrioventricular septum (*) and the deep infolding of the atrial wall superior to the floor of the oval fossa (dotted lines). The true septal area is considerably smaller. (b) The cardiac base (short axis) is dissected by removing most of the atrium's aspects. The right pectinate muscles skirt around the vestibule of the right atrium and reach the orifice of the coronary sinus. Note that the pectinate muscles in the LA are limited mostly within the appendage and the dotted line marking the vestibule of the mitral annulus. CSo, coronary sinus orifice; ICV, inferior caval vein; LAA, left atrial appendage; PA, pulmonary artery; RAA, right atrial appendage.

may result in hemopericardium in a highly anticoagulated patient because blood will dissect the vascularized fibro-fatty tissue that is sandwiched between the right and left atrial myocardium at this level [47–49].

The major part of the endocardial LA including the septal and interatrial groove component is relatively smooth walled. The left aspect of the interatrial groove, apart from a small crescent-like edge, is almost indistinguishable from the parietal atrial wall. The smoothest parts are the superior and posterior walls, which make up the pulmonary venous component, and the vestibule surrounding the mitral orifice. Behind the posterior portion of

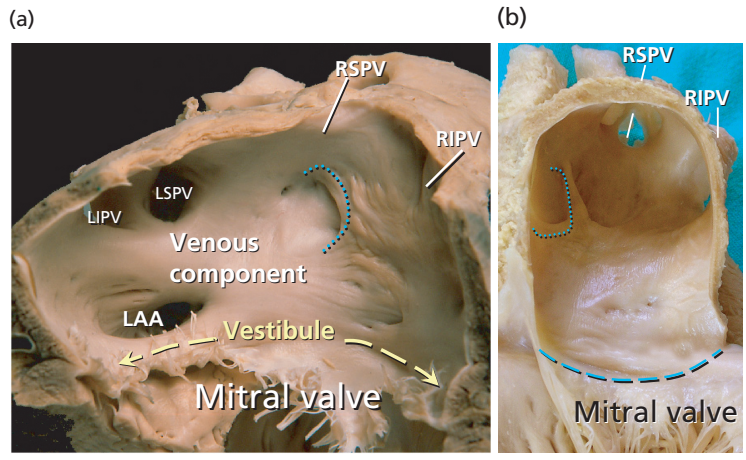

Figure 1.3 (a) Dissection of the posterior wall of the LA close to Waterston's groove. The smooth-walled venous component of the LA is the most extensive. The septal aspect of the LA shows the crescentic line of the free edge (dotted line) of the flap valve against the rim of the oval fossa. (b) The orifices of the right superior and inferior pulmonary veins (RSPV and RIPV) are adjacent to the plane of the septal aspect of the LA (dotted line). The dashed blue line marks the hinge of the mitral valve. LAA, left atrial appendage; LIPV, left inferior pulmonary vein; LSPV, left superior pulmonary vein.

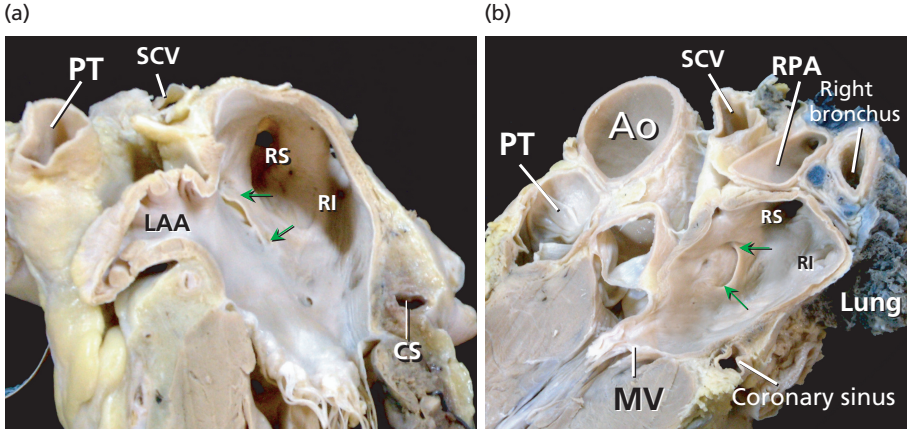

Figure 1.4 Longitudinal sections through the left atrial appendage (LAA) showing the orifices of the right PV; the flap valve of the oval fossa overlaps (arrows) the rim to form the septal aspect of the LA. Note the relation of the superior caval vein (SCV) to the right superior pulmonary vein (RS). (b) Longitudinal section to show the relationship of the roof of the left atrium with the right pulmonary artery (RPA) and right bronchus. Ao, aorta; CS, coronary sinus; MV, mitral valve; PT, pulmonary trunk; RI, right inferior pulmonary vein; RS, right superior pulmonary vein.

the vestibular component of the LA is the anterior wall of the coronary sinus [41] (Figures 1.3 and 1.4).

The walls of the left atrium and the septum

The left atrial wall and its thickness

The walls of LA, excluding the LAA, can be described as anterior, superior, left lateral, septal, and posterior. The anterior wall is located behind the ascending aorta and the transverse pericardial sinus. From epicardium to endocardium its width is 3.3 ± 1.2 mm (range 1.5–4.8 mm) in unselected necropsic heart specimens, but this wall can become very thin at the area near the vestibule of the mitral annulus where it measures an average of 2 mm in thickness in our autopsy studies. The roof or superior wall of the LA is in close proximity to

the right pulmonary artery and its width ranges from 3.5 to 6.5 mm (mean 4.5 ± 0.6 mm). The thickness of the lateral wall ranges between 2.5 and 4.9 mm (mean 3.9 ± 0.7 mm) [41].

As already stated, an anatomic septum is like a wall that separates adjacent chambers so that perforation of a septal wall would enable us to enter from a chamber to the opposite one without exiting the heart. Thus, the true atrial septal wall is confined to the flap valve of the oval fossa. The flap valve is hinged from the muscular rim that, deriving from the septum secundum, is seen from the right atrial aspect of the interatrial wall. At its anteroinferior portion the rim separates the foramen ovale from the coronary sinus and the vestibule of the tricuspid valve [48] (Figure 1.2). On the left atrial aspect there is no visible rim and the flap valve overlaps the oval rim quite considerably and two horns mark the usual site of fusion with the rim (Figure 1.3 and 1.4). The measurement of the mean thickness of the atrial septum in normal hearts at the level of the anteroinferior portion of the muscular rim is 5.5 ± 2.3 mm, and the mean thickness of the flap valve is 1.5 ± 0.6 mm [41]. These results agree with previously published echocardiographic studies [50]. The major portion of the rim around the fossa is an infolding of the muscular atrial wall that is filled with epicardial fat. Superiorly and posteriorly there is an interatrial groove, also known as Waterston's groove, whose dissection permits the separation of the right and left atrial myocardial walls and to enter the LA without transgressing into the right atrium. Anteriorly and inferiorly, the rim and its continuation into the atrial vestibules overlies the myocardial masses of the ventricles from which they are separated by the fat-filled inferior pyramidal space [48,51] (Figures 1.2–1.4).

The posterior wall of the LA is a target of currently used ablation procedures in patients with AF. Early surgical interventions aimed at reducing the critical mass of atrial tissues created long transmural linear lesions incorporating the posterior LA wall. The posterior wall of the LA is related to the esophagus and its nerves (vagal nerves) and the thoracic aorta, and its inferior portion is related to the coronary sinus. In a previous study in 26 unselected human heart specimens the overall thickness of the posterior LA wall was 4.1 ± 0.7 mm (range 2.5–5.3 mm) [41]. In a subsequent study we measured the thickness of the posterior wall from the epicardium to endocardium, obtaining sagittal and transverse sections through the LA at three levels (superior, middle, and inferior close to the coronary sinus) in three different LA regions (right venoatrial junction, mid-posterior atrial wall, and left venoatrial junction) [52]. We also analyzed the myocardial content of the LA wall at all these predefined sites. The region with the thickest myocardial content was the mid-posterior LA wall (2.9 ± 0.5 mm, range 0.6–4.2 mm). The inferior level, immediately superior to the coronary sinus and between 6 and 15 mm from the mitral annulus, had the thickest posterior LA wall (6.5 ± 2.5 mm, range 2.8–12 mm). The latter thickness was due to a rather bulky myocardial layer (4.3 ± 0.8 mm) and the presence of a profuse amount of fibro-fatty tissue, both components being less developed at more superior levels of the posterior LA wall. The wall at the plane of the right or left venoatrial junction had the thinnest musculature (2.2 ± 0.3 mm, range 1.2–4.5 mm) and a very scanty content of fibro-fatty tissue [52]. In some samples of histological sections obtained at the PV and posterior atrial wall, the myocardial layer had small areas of discontinuities that were filled with fibrous tissue [42,53].

The myoarchitecture of the left atrial wall

Detailed dissections of the subendocardial and subepicardial myofibers along the entire thickness of the LA walls have shown a complex architecture of overlapping bands of aligned myocardial bundles [41,51] (Figures 1.5 and 1.6). The term "fibers" describes the macroscopic appearance of strands of cardiomyocytes. These fibers are circumferential when they run parallel to the mitral annulus and longitudinal when they are approximately perpendicular to the mitral orifice. Although there are some individual variations, our epicardial dissections of the LA have shown a predominant pattern of arrangement of the myocardial fibers [41]. On the subepicardial aspect of the LA, the fibers in the anterior wall consisted of a main bundle that was parallel to the atrioventricular groove. This was the continuation of the interatrial bundle (Bachmann's bundle) [54], which could be traced rightward to the junction between the right atrium and the superior caval vein. In the LA, the interatrial bundle

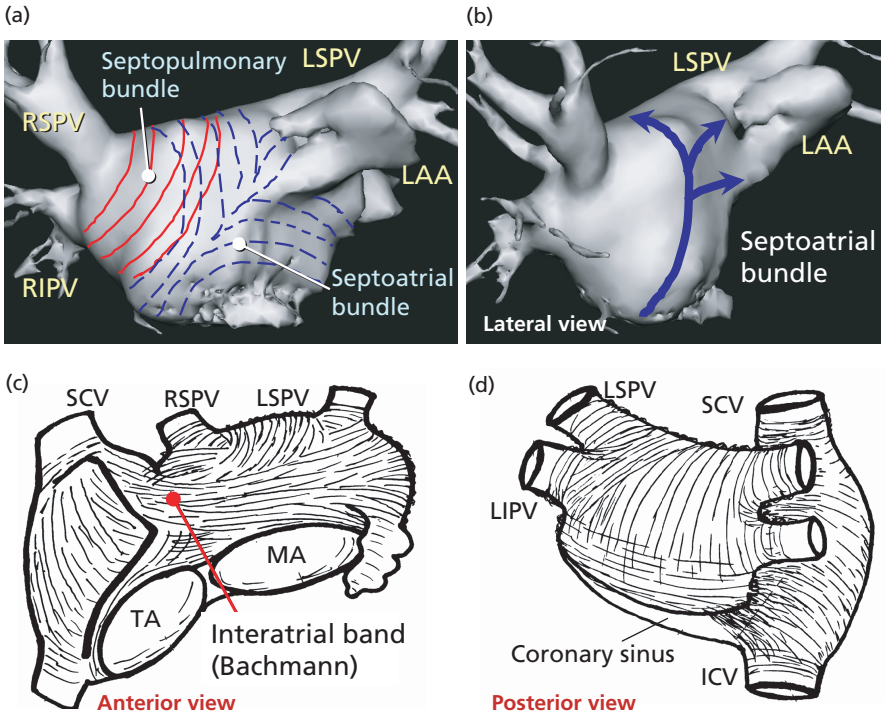

Figure 1.5 Schematic representation of the general arrangement of the subepicardial and subendocardial fibers of the LA, viewed from the anterior (a, c) and posterior (b, d) aspect. (b) Note the three major subendocardial fascicles of the septoatrial bundle. ICV, inferior caval vein; LAA, left atrial appendage; LIPV, left inferior pulmonary vein; LSPV, left superior pulmonary vein; MA, mitral valve; RIPV, right inferior pulmonary vein; RSPV, right superior pulmonary vein; SCV, superior caval vein; TA, tricuspid valve.

was joined inferiorly at the septal raphe (the portion that is buried in the atrial septum) by fibers arising from the anterior rim of the oval foramen. Superiorly, it blended with a broad band of circumferential fibers that arose from the anterosuperior part of the septal raphe to sweep leftward into the lateral wall. Reinforced superficially by the interatrial bundle, these circumferential fibers passed to either side of the neck of the atrial appendage to encircle the appendage, and reunited as a broad circumferential band around the inferior part of the posterior wall to enter the posterior septal raphe (Figures 1.5 and 1.6). The epicardial fibers of the superior wall are composed of longitudinal or oblique fibers, (named by Papez as the "septopulmonary bundle" in 1920) [55] that arise from the anterosuperior septal raphe, beneath the circumferential fibers of the Bachmann's bundle. As they ascend the roof, they fan out to pass in front, between, and behind the insertions of the pulmonary veins and the myocardial sleeves that surround the venous orifices. On the posterior wall, the septopulmonary bundle often bifurcates to become two oblique branches. The leftward branch fused with, and was indistinguishable from, the circumferential fibers of the anterior and lateral walls, whereas the rightward branch turned into the posterior septal raphe. Often, extensions from the rightward branch passed over the septal raphe to blend with right atrial fibers and others toward the septal mitral valve annulus, forming a line that marked an abrupt change in subendocardial fiber orientation.

On the subendocardial aspect of the LA, most specimens showed a common pattern of general architecture. The dominant fibers in the anterior wall were those orginating from a bundle described by Papez as the septoatrial bundle [55]. The fibers of this bundle ascended obliquely from the anterior interatrial raphe and combined with longitudinal fibers arising from the vestibule. They passed the posterior aspect of the LA between the left and right pulmonary veins, blending with longitudinal

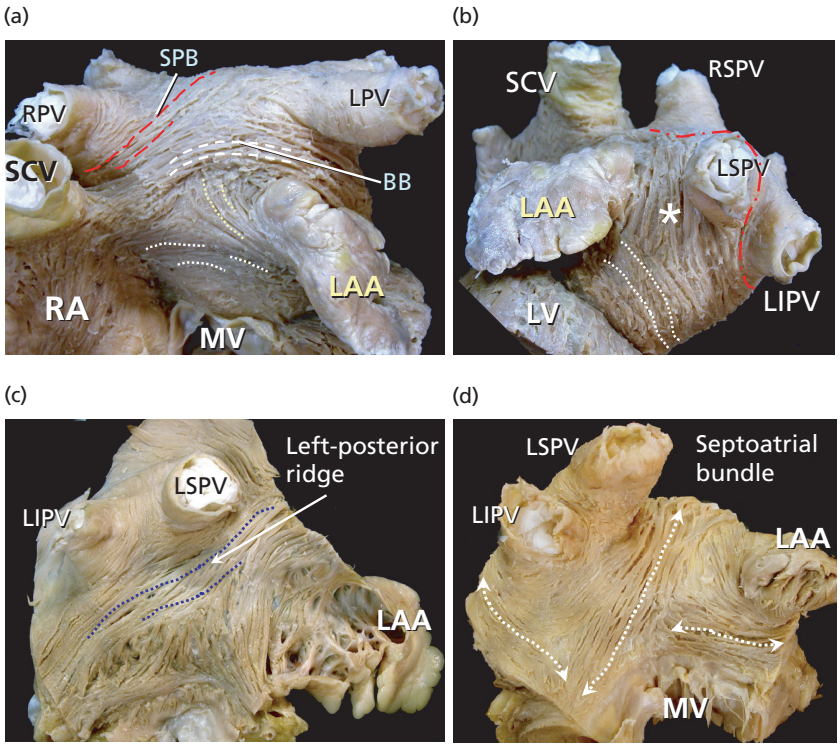

Figure 1.6 (a, b) Dissections of the subepicardial fibers viewed from the anterior and left lateral aspects. The interatrial (Bachmann) bundle (BB, white dashed lines) crosses the septal raphe and blends into the circumferential fibers of the anterior wall (dotted lines), passes to either side of the neck of the atrial appendage and runs parallel to the posterolateral aspect (*) of the LA. Oblique fibers of the septopulmonary bundle (SPB) become longitudinal as they cross the roof between the left and right PVs (red dashed lines). (c, d) The left atrium everted to show the subendocardial fibers and the fiber arrangement of the septoatrial bundle and its three major fascicles (double-headed arrows). Note that endocardially the myocardial content of the left posterior ridge is the prolongation of leftward fibers from the septoatrial bundle that run toward the orifices of the left-sided PVs and the mouth of the left atrial appendage (LAA, blue dotted lines). LIPV, left inferior pulmonary vein; LPV, left pulmonary vein; LSPV, left superior pulmonary vein; LV, left ventricle; MV, mitral valve; RA, right atrium; RPV, right pulmonary vein; RSPV, right superior pulmonary vein; SCV, superior caval vein.

or oblique fibers of the septopulmonary bundle from the subepicardial layer. The septoatrial bundle also passed leftward, superior and inferior to the mouth of the atrial appendage to reach the lateral and posterior walls. Some of these fibers encircled the mouth of the LA appendage and continued into the pectinate muscles within the appendage (Figures 1.5 and 1.6). The subendocardial fibers at the orifices of the PVs were usually loop-like extensions from the longitudinal fibers. These fibers became circular at varying distances into the venous walls and were continuous with the subepicardial fibers. In some specimens, however, the subendocardial fibers were longitudinal or oblique, whereas the subepicardial fibers were circular, or vice versa. The distal margins of the muscular sleeves were highly irregular in the majority of veins.

Pulmonary veins and their ending into the left atrium

Clinical imaging studies using magnetic resonance imaging (MRI) and multislice computed tomography (CT) demonstrated the complex anatomy of the PVs with significant variability in dimensions, shape, and branching patterns [56–63]. When assessed in a correct attitudinal orientation, the left PVs are located more superiorly than the right-sided veins [64] (Figure 1.7). The superior PVs run cranially and more anteriorly, whereas the

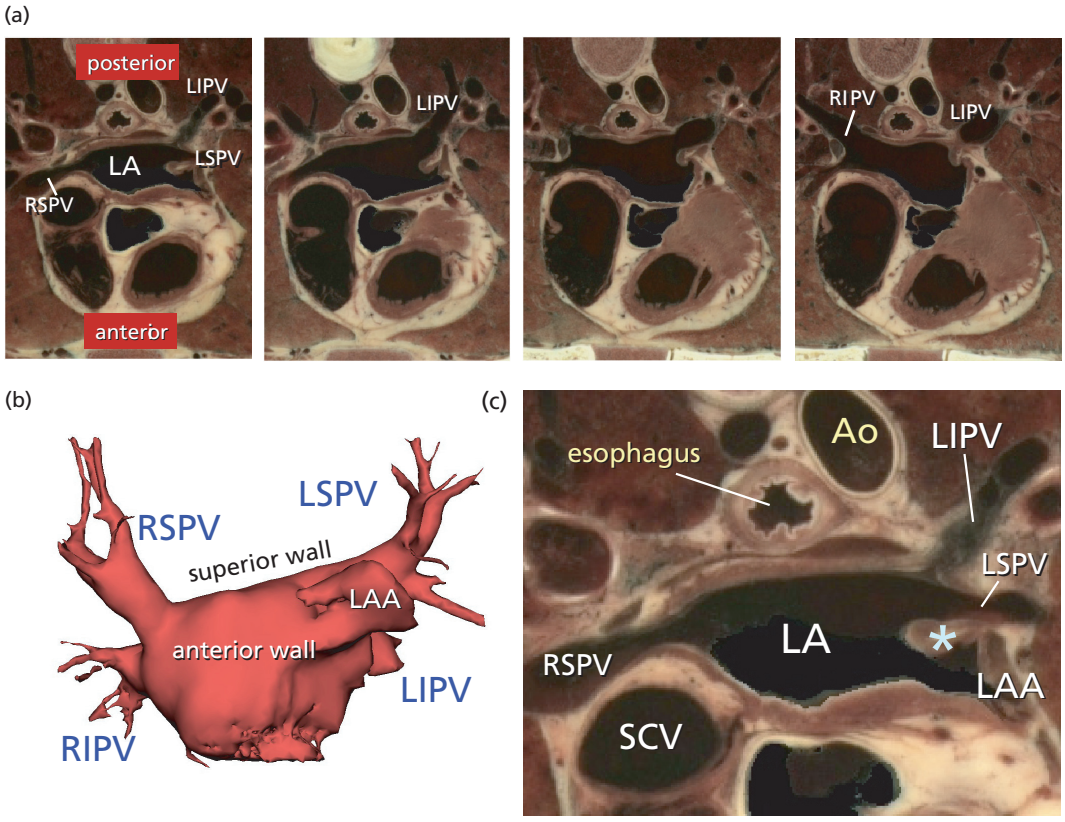

Figure 1.7 Left atrial anatomy as depicted on axial slices obtained with the "Visible Human Slice and Surface Server" [46] and three-dimensional reconstruction of the left atrium (LA) and pulmonary veins (PV) using the NavX® system from data obtained with a 32-slice multidetector CT scanner. (a) Four successive slides obtained from a cranial to caudal direction. Note that the left PVs are located more superiorly than the right-sided veins. The superior PVs run cranially and more anteriorly and the inferior veins have a more posterior and lateral course. (b) The NavX system allows better geometric visualization of the LA, left atrial appendage (LAA), and PVs in a correct attitudinal orientation. The LAA is anterior to the left superior PV (LSPV). (c) The right superior PV (RSPV) is seen behind the superior caval vein (SCV). Note the posterior wall of the LA related to the esophagus and aorta and the infold (*) of the posterolateral atrial wall protuding into the endocardial LA surface as a prominent ridge. Ao, aorta; LIPV, left inferior pulmonary vein; RIPV, right inferior pulmonary vein.

inferior veins have a more posterior and lateral course. The right superior PV runs near the posterior aspect of the right atrium immediately behind the superior caval vein. The right PVs are also related to the right pulmonary artery, which passes close to the roof of the LA [46] (Figure 1.8).

The orifices of the right PVs are directly adjacent to the plane of the atrial septum (see Figures 1.3 and 1.4). The left superior PV lies superiorly and posteriorly to the mouth of the LAA, separated endocardially by a posterolateral ridge which, epicardially, is a fold that frequently extends to the origin of the left inferior PV [41,46,61–63]. Although textbooks typically depict four venous orifices, anatomic observations confirmed by MRI and CT studies in structurally normal hearts, have demonstrated the variability of the ending of the PVs into the LA. In our series of 35 postmortem human hearts, we found 26 specimens (74%) with two PVs on each side [44]. Of these 26 hearts, 15 (69%) had four separate openings of the PVs into the LA and the remaining 11 specimens (31%) had a "vestibule-like" portion for both PVs before opening via a common orifice into the atrium (Figures 1.9 and 1.10). The venous vestibule is more frequently found on the left than on the right side and its length ranged from 3 to 15 mm (7 ± 3 mm). A single common PV, defined as a vein branching at the

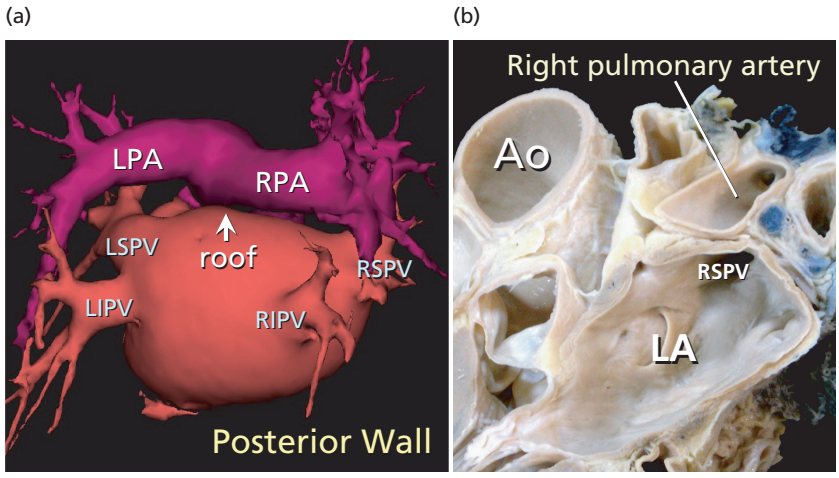

Figure 1.8 (a, b) The right superior pulmonary vein (RSPV) is related to the right pulmonary artery (RPA) that passes close to the roof of the left atrium (LA). Ao, aorta; LIPV, left inferior pulmonary vein; LPA, left pulmonary artery; LSPV, left superior pulmonary vein; RIPV, right inferior pulmonary vein.

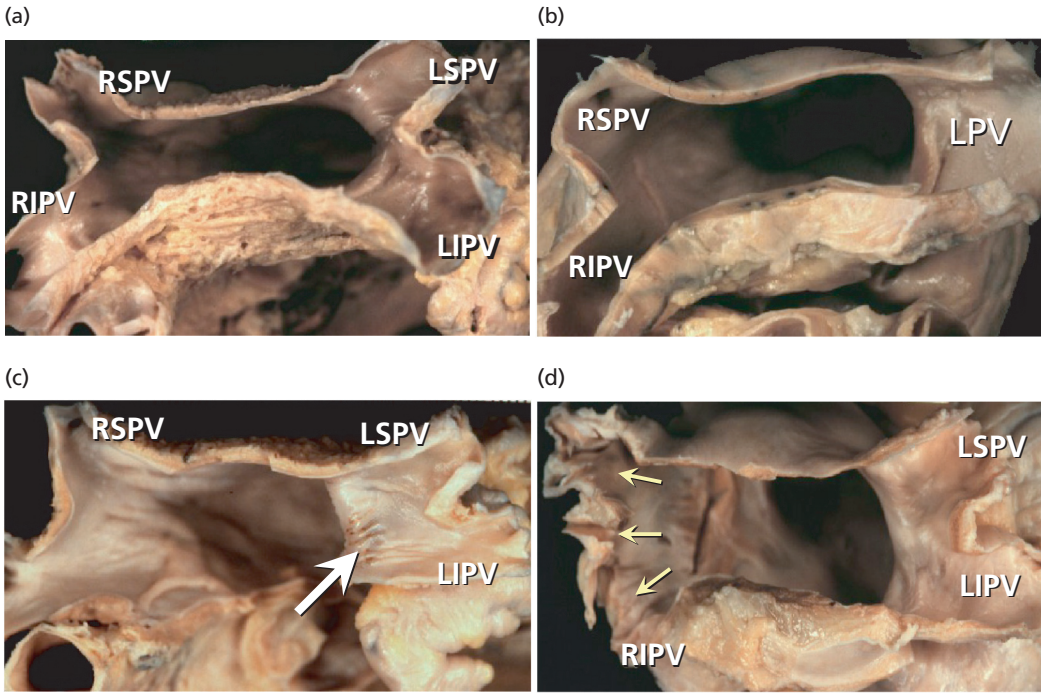

Figure 1.9 Four heart specimens sectioned tranversally with the roof of the LA removed and viewed from above to shows the entrance of the pulmonary veins (PVs). (a) The arrangement of four individualized ending of the PVs into the LA. (b) A single left PV (LPV). (c) Four PVs; the left PV has a "vestibule-like" portion (white arrow) for both the left superior PV (LSPV) and left inferior PV (LIPV) before opening via a common orifice into the left atrium. (c) This heart displayed more than four PVs: three orifices on the right (yellow arrows) and two on the left. RIPV, right inferior pulmonary vein; RSPV, right superior pulmonary vein.

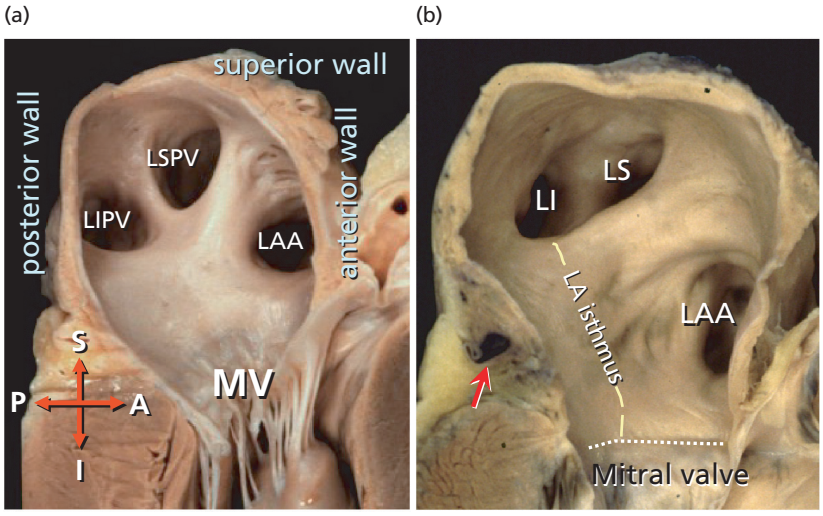

Figure 1.10 Longitudinal sections of two hearts illustrating endings of the pulmonary veins (PVs) into the LA. (a) An individualized ending of the left superior PV (LSPV) and the left inferior PV (LIPV) into the LA. The left PVs lie superior and posterior to the mouth of the left atrial appendage (LAA), both separated by a muscular fold. (b) Heart showing a common vestibule for both left PVs. Note the larger anteroposterior diameter than the superoinferior one and the line connecting the inferior margin of the ostium of the left inferior PV to the mitral annulus called the left atrial isthmus. The red arrow marks the coronary sinus. LI, left inferior PV; LS, left superior PV; MV, mitral valve.

level of the hilum of the lung, was found in three hearts (9%), two on the left side and one on the right. Six hearts (17%) displayed more than four pulmonary veins (three orifices on the right and two on the left). Clinical examination demonstrated four venous orifices in 81% of patients, while 3% had three orifices and 16% had five orifices [59]. The most common variation is a separate origin of the vein coming from the right middle lobe of the lung (Figure 1.9). The distance between the orifices of the right PVs ranged from 3 to 14 mm (mean 7.3 ± 2.7 mm), and in the left PVs from 2 to 16 mm (mean 7.5 ± 2.8 mm). A thin inter-orifice left atrial rim between the superior and inferior PVs (measuring from 1 to 3 mm) was found in 50% of the hearts. Endocardial examination of the LA using three-dimensional MRI has shown that the shortest distance between the right and left PVs, the so-called roof line, was 29.9 ± 5.9 mm, ranging between 18.9 and 39.2 mm [62].

Anatomic studies and clinical imaging investigations have shown that the PV ending in the LA is not perfectly cylindrical but has a funnel-shaped morphology, making it difficult to identify a sharp landmark for the anatomic limits of the PV ostium [41,56,57]. Discounting the common vestibule, the diameter of the venous orifices at the venoatrial junction ranged in our anatomic specimens from 8 to 21 mm (12.5 ± 3 mm). The transversal diameter of the common vestibule is longer than its superoinferior diameter (19.5 ± 3 mm vs.13.5 ± 1 mm) [41]. Early studies demonstrated a strong correlation between the degree of left atrial dilation and both occurrence and duration of AF [65]. Imaging studies of the PVs demonstrated that the ostial diameters of the superior PV were greater in patients with AF than in controls [60,66].

Gross anatomy of the left posterolateral ridge

The posterolateral ridge between the orifices of the left PVs and the mouth of the LAA is the most relevant structural prominence of the endocardial LA (Figure 1.11). Although already described in 1907 by Arthur Keith [67] as the "left tænia terminalis" (terminal band or strip) and 13 years later by James Papez [55] as the "left posterior crest", the LA posterolateral ridge actually is a fold of the posterolateral left atrial wall protruding into the endocardial LA surface as a prominent crest or ridge (Figure 1.11). Epicardially, this broad bundle is in continuity with the uppermost and distal part of the interatrial band (Bachmann's bundle).

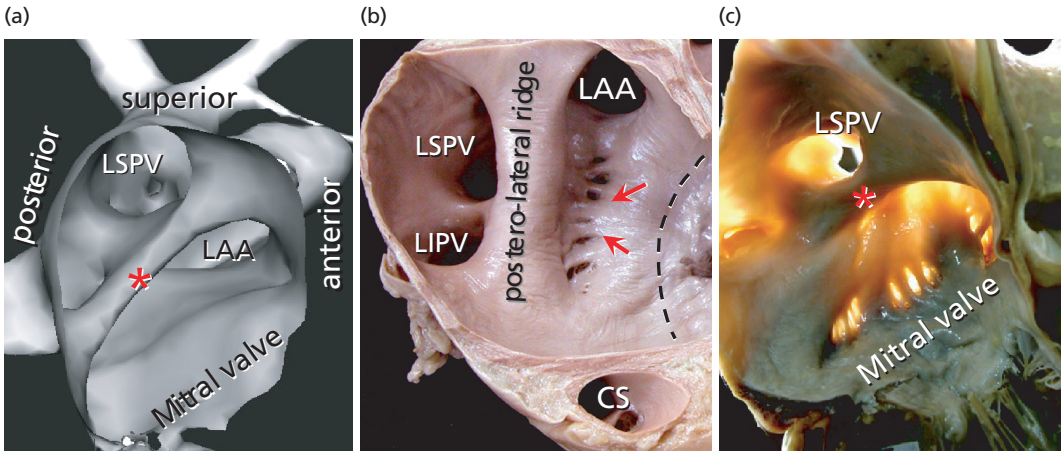

Figure 1.11 Endocardial visualization of the left posterolateral wall. (a) Three-dimensional reconstruction of the endocardial left atrium using the NavX system from data obtained with a 32-slice multidetector CT scanner. Note the prominent posterolateral ridge (*) between the left atrial appendage (LAA) and the left superior pulmonary vein (LSPV) along the lateral wall from its anterosuperior to posteroinferior region. (b, c) Two postmortem heart specimens showing prominent endocardial posterolateral ridges, extending in (b) to the inferior margin of the left inferior pulmonary vein (LIPV). Observe the muscular trabeculations extending inferiorly from the left appendage to the vestibule of the mitral valve (red arrows). (c) Transillumination of the left lateral wall to illustrate the extra-appendicular posterior pectinate muscle and the thinnest muscular wall in between the muscular trabeculae. CS, coronary sinus.

Endocardially, the myocardial content is the prolongation of leftward fibers from the septoatrial bundle that run toward the orifices of the left-sided PVs and the mouth of the LAA (see Figure 1.6). The shape and size of this posterolateral LA ridge is of relevance during catheter ablation of AF when encircling the orificies of the left PVs or during ablation of extrapulmonary vein triggers arising around or inside the LAA. Anatomic information of this structure may be useful in order to perform ablation techniques more efficiently and safely, and it can be obtained with current multislice CT and MRI reconstructions of the endocardial aspect of the LA [61–63]. The ridge extends along the lateral wall of the LA from the anterosuperior to posteroinferior region. A recent three-dimensional MRI study showed that the ridge was narrowest between the left superior PV and the LAA in 84% of patients. In this study, the mean distance between the left superior PV and the LAA, and between the left inferior PV and the LAA, were found to be 3.8 ± 1.1 mm and 5.8 ± 2.0 mm, respectively. The ridge was narrower than 5 mm in the majority of patients, thus determining the possibility of obtaining stable catheter position in this region [61]. Our recent anatomic study of 32 structurally normal human heart necropsic specimens also revealed a thicker myocardial wall of the ridge at its inferior level adjacent to the inferior PV, with a range between 1.5 and 4.2 mm (mean 2.8 ± 1.1 mm). The mean length of the ridge was 24.2 ± 5.3 mm (range 14.2–32.5 mm) with a constant superior insertion at the lateral roof of the LA extending inferiorly to reach the posteroinferior margin of the inferior PV in 88% of hearts (unpublished observations). A CT scan study showed a prominent ridge in all subjects extending from the superior part of the left superior PV to the inferior PV in 70–72% of patients [63]. These investigators also found no significant differences in the length and width of the ridge between patients with AF and controls [63].

Gross anatomy of the left atrial appendage

The LAA is characteristically a small finger-like extension of the LA with a multilobulated appearance in 80% of hearts [68,69] (Figure 1.12). A quantitative study of the normal LAA in 500 autopsy hearts showed that the mean length, width, and size of the appendage increased with age up 20 years [69]. In adult postmortem hearts the mean orifice

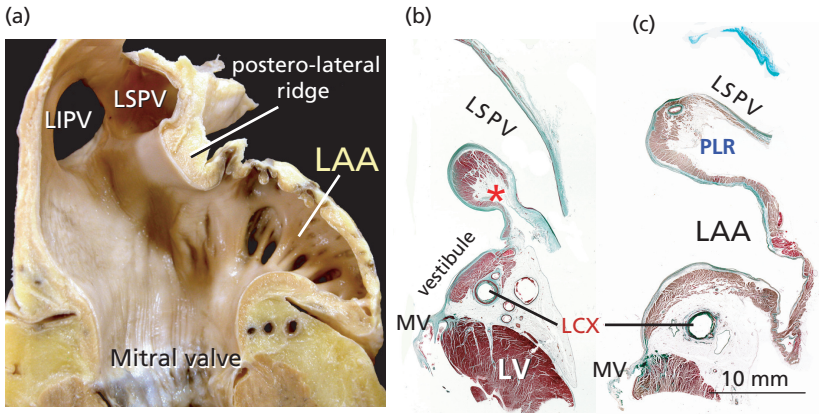

Figure 1.12 (a) Longitudinal section through left atrial appendage (LAA) showing the orifices of the left pulmonary veins, and the left posterolateral ridge. (b, c) Longitudinal sections through the left superior pulmonary vein (LSPV) and left atrial appendage (LAA) and left superior pulmonary vein (LSPV) stained with Masson's trichrome. Note the myocardium and fat tissue (*) of the posterolateral ridge and the left circumflex artery (LCX) closer to the vestibule of the left atrium in (b). LIPV, left inferior pulmonary vein; LV, left ventricle; MV, mitral valve; PLR, posterolateral ridge.

diameter of the LAA was 1.07 cm in women and 1.16 cm in men, in contrast with morphological examinations of LAA orifices using CT scans that showed a mean longitudinal and transverse diameter of 3.2 ± 0.6 mm and 1.9 ± 0.5 mm, respectively [63,69]. The greater diameters in the in vivo human studies as compared to necropsic measurements most likely is due to tissue retraction produced by the fixation of the specimens in the latter studies. The LAA orifice and volume of patients with AF is greater than that observed in controls.

Reinforced superficially by the interatrial bundle, circumferential fibers that arise from the anterosuperior part of the septal raphe pass to either side of the neck of the left appendage to form broad bundles of muscular connections between the appendage and the body of the LA. A recent study has shown that to electrically disconnect the LAA it is necessary to apply long-lasting radiofrequency pulses that gradually change the activation sequence, thus suggesting a dense circumferential connection of the appendage to the LA [32]. A narrow, oval-shaped mouth marks the junction between the LAA and the venous component of the LA. The myocardial ridge and an inflection of the endocardial surface bounded the ostial borders of the appendage in most hearts. In the LA, the pectinate muscles are mostly confined within the left appendage. They form a complicated network of muscular strips lining the endocardial surface. In some 28% of our human heart specimens the anterior ostial margin of the appendage does not present as a clear-cut border and muscular trabeculations can be found extending inferiorly from the appendage to the vestibule of the mitral valve (see Figure 1.11). These extra-appendicular myocardial bands correspond to the small posterior set of pectinate muscles originating from the septoatrial bundle to embrace the left appendage. In those hearts with extra-appendicular posterior pectinate muscles, the areas in between the muscular trabeculae had the thinnest muscular walls (0.5 ± 0.2 mm) (see Figures 1.6 and 1.11). In other specimens (15%), remnants of pectinate muscles between the ostium of the left inferior PV and vestibule of the mitral annulus can be found. A previous histological study of the mitral isthmus described "small isthmus crevices" present in almost all patients that may entrap the tip of the ablation catheter, which may lead to excessive tissue heating and tamponade.

The left circumflex coronary artery runs epicardially in the fat-filled atrioventricular groove, related to the smooth anterior vestibule and in close proximity to the inferior border of the orifice of the LAA (Figure 1.12). The shortest distance from the left appendage orifice and the circumflex artery was < 3–5 mm in 80% of our unselected human heart necropsic specimens. In CT in vivo studies the left circumflex coronary artery ran < 2 mm from the LAA orifice in 74% of cases, an anatomic detail to

be considered when ablating inside or around the orifice of the LAA.

Architecture of the left posterolateral ridge: the Marshall structures

The posterolateral ridge is more than a simple endocardial fold of the lateral LA wall that influences the stability of the contact of the tip of the catheter with the endocardium during an ablation procedure. Electrophysiological and surgical investigations demonstrated extra-PV atrial foci after PV isolation originating from the LAA [22,32]. In addition, the junctional area between the LAA and the LA body has a relevant impact on the fibrillatory process, acting as a source of activity spreading to the rest of the atrium and contributing to the maintenance of atrial fibrillation [19,21–23, 70–72]. Because of the potential relevance for current and future endocardial catheter ablation techniques we will describe the architectural arrangement of myocardial bundles forming the posterolateral LA ridge and its vascular and autonomic nervous system content, as well as the anatomic relations with the Marshall structures (the oblique vein and ligament).

The so-called oblique vein of Marshall is part of the ligament of Marshall (LOM), formed by the venous element and fibro-fatty tissue, muscular bundle and autonomic nerves, all forming a vestigial fold of the pericardium described by John Marshall in 1850 [73] (Figure 1.13). The LOM courses obliquely above the LAA and can be traced laterally to the left superior PV bundle in the epicardial aspect of the left atrial fold that forms the left posterior "crest". Sherlag et al. [74] first demonstrated the existence of muscular left atrial "tracts" within this vestigial fold and found electrical activity arising from the LOM. In their study, Sherlag et al. recorded double potentials from the ligament, advancing the hypothesis that this structure could play a role in arrhythmogenesis [74]. More recently, the so-called Marshall bundles have been thought to be the origin of certain forms of focal AF and that a considerable percentage of non-pulmonary vein foci may arise from the LOM [30,31,75–79]. Electroanatomic mapping showed a common pattern of electrical connection between the LOM and coronary sinus muscular sleeves, resulting in early activation of the low posterolateral wall of the LA. In addition, some patients had distal electrical connections at the floor of the left inferior PV or anterolateral wall of the left superior PV [75,76].

In an elegant histological examination, Kim et al. [80] demonstrated multiple myocardial "tracts" present within the LOM that directly insert into the coronary sinus musculature near the origin of the vein of Marshall or distally into the posterior free wall of the LA. They found in 57% of specimens both superficial and deep muscular "tracts" in

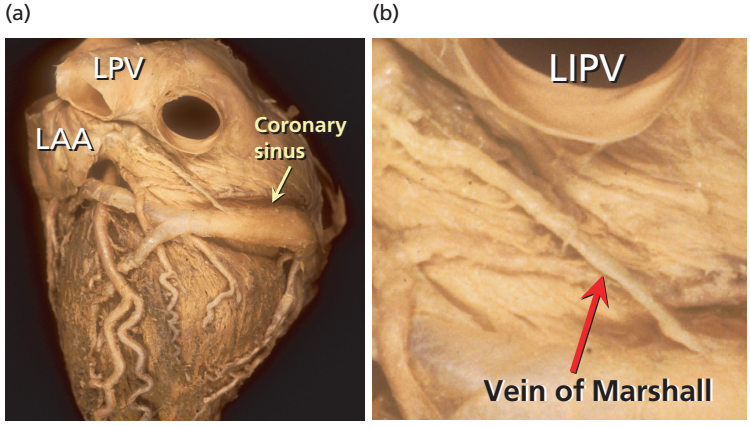

Figure 1.13 (a) Heart specimen showing the spatial relationship of the coronary sinus and the vein/ligament of Marshall. The coronary sinus runs along the epicardial portion of the vestibular component of the LA surrounding circumferentially the orifice of the mitral valve. (b) Note in the enlarged figure, the left atrial oblique vein of Marshall formed by the venous element with fibro-fatty tissue and small muscular bundles. LAA, left atrial appendage; LIPV, left inferior pulmonary vein; LPV, left pulmonary vein.

relation to the oblique vein of Marshall with an overall mean length and diameter of 7.8 ± 3.9 mm and 0.7 ± 0.2 mm, respectively. Electrical activity originating from the LOM can be recorded from the endocardial aspect of the LA in or around the orifices of the left PV. A recent anatomic study showed that Marshall bundles gradually diminished in density towards the distal venous branch and reached the left inferior PV–LA junction and left superior PV–LA junction in 76% and 24% of cases, respectively [81]. In patients with AF undergoing ablation of the LOM, it has been shown that most arrhythmic episodes arise from the distal segment of the ligament close to the left superior PVs [75,77,79]. An angiographic study also revealed that the distal end of the vein of Marshall and its branches are likely to be distributed around the left superior PV or the left inferior PV ostia, especially in patients with arrhythmogenic foci [79]. Studies of endocardial ablation to eliminate activation from Marshall bundles recognize that the most frequently successful ablation site is at the inferior border of the ostium of the left inferior PV. We have studied the Marshall structures, demonstrating that they course along the left posterior ridge and that they are in close proximity to the endocardial aspect of the left atrium (Figure 1.14). In 73% of specimens the oblique vein of Marshall or its ligament runs at a distance less than 3 mm from the superior level of the endocardial ridge. Throughout the trajectory of the vein in relation to the left posterior ridge, we observed in all specimens small muscular bundles that crossed the oblique vein to connect with the left atrial free wall.

The Marshall ligament is richly innervated by sympathetic nerve fibers [80,81]. Adrenergic

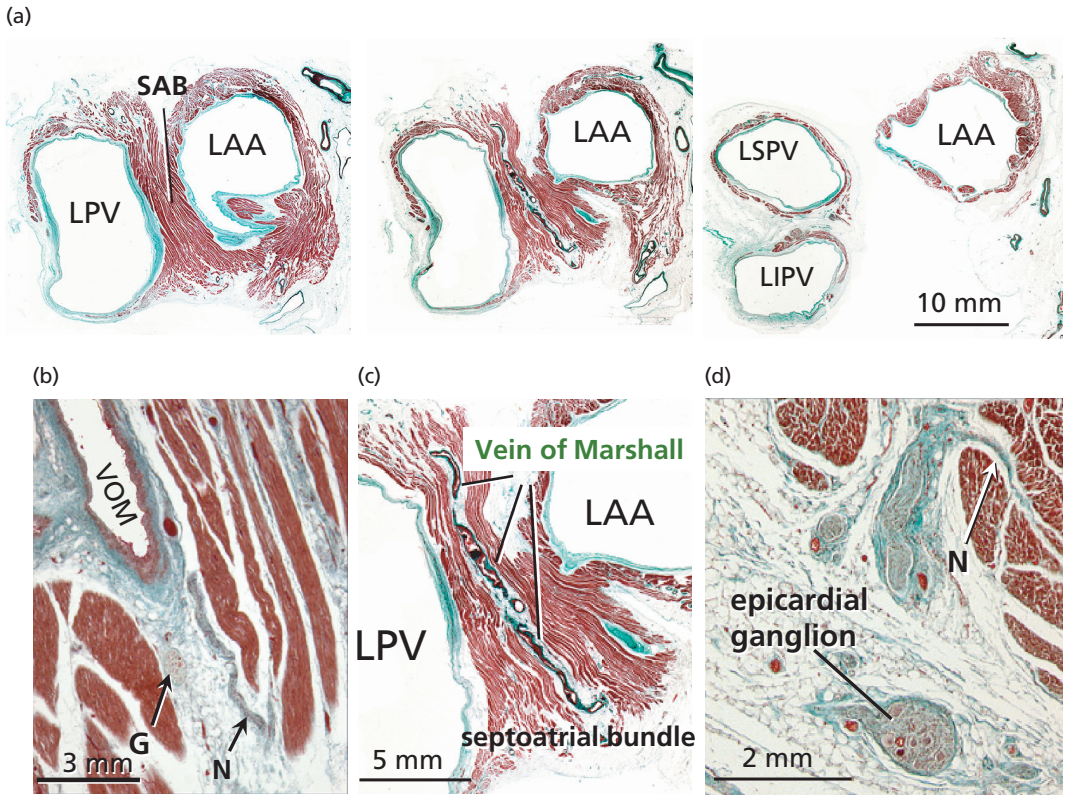

Figure 1.14 (a) Transverse sections at different levels of the myocardial sleeve of the left pulmonary vein (LPV), septoatrial bundle (SAB), and left atrial appendage (LAA) from a 56-year-old man. (b) Transverse section showing the oblique vein of Marshall (VOM). The arrows (G) and (N) indicate the ganglion and nerve bundles in the vicinity of the vein, respectively. (c) An enlargement of the septoatrial bundle shown in (a). Note that the VOM was found in direct contact with the myocardium of the septoatrial bundle. (d) Transverse section showing the epicardial ganglion and nerve bundles (N) in the vicinity of the myocardium of the septoatrial bundle. (Trichrome stain.) LIPV, left inferior pulmonary vein; LSPV, left superior pulmonary vein.

sensitivity of the myocardial tissues within the LOM may be responsible for atrial tachyarrhythmias arising from the LA [78]. Both focal sources arising from Marshall structures and muscular connections with the epicardial interatrial Bachmann's bundle and the inner septoatrial bundle may have implications in the fibrillatory process and spread of AF activity between both atria (Figure 1.14). Recent reports have shown that left-to-right interatrial conduction occurs predominantly through the Bachmann bundle and that sinus impulses propagated through this interatrial bundle could excite the Marshall musculature and the nearby left atrium simultaneously [82,83].

The left atrial isthmus

Linear ablation connecting the inferior margin of the ostium of the left inferior PV to the mitral annulus appears to increase the success rate of catheter ablation in patients with AF [13,84]. Although this posteroinferior wall of the LA between the orifice of the left inferior PV and the mitral annulus cannot be considered an anatomic entity, it is being named by electrophysiologist as the left atrial isthmus or mitral isthmus (Figure 1.15). In a recent anatomic study of 20 hearts, Anton Becker [85] showed marked variability in the dimensions of the mitral isthmus with considerable differences in thickness of the left atrial myocardium at various levels and among different hearts. This study also showed the close anatomic relation between the isthmus area with the great cardiac vein and the left circumflex artery. The mean distance between the left inferior PV and the mitral annulus ranged between 17 and 51 mm (mean 34.6 mm). In some hearts the left atrial myocardium extended into the atrial aspect of the mitral valve leaflets. Gaps in the lesion line may result in conduction delay and facilitate left atrial flutter. Therefore, the variable thickness of the left atrial myocardial tissue is highly relevant to achieving an adequate transmural linear lesion across the

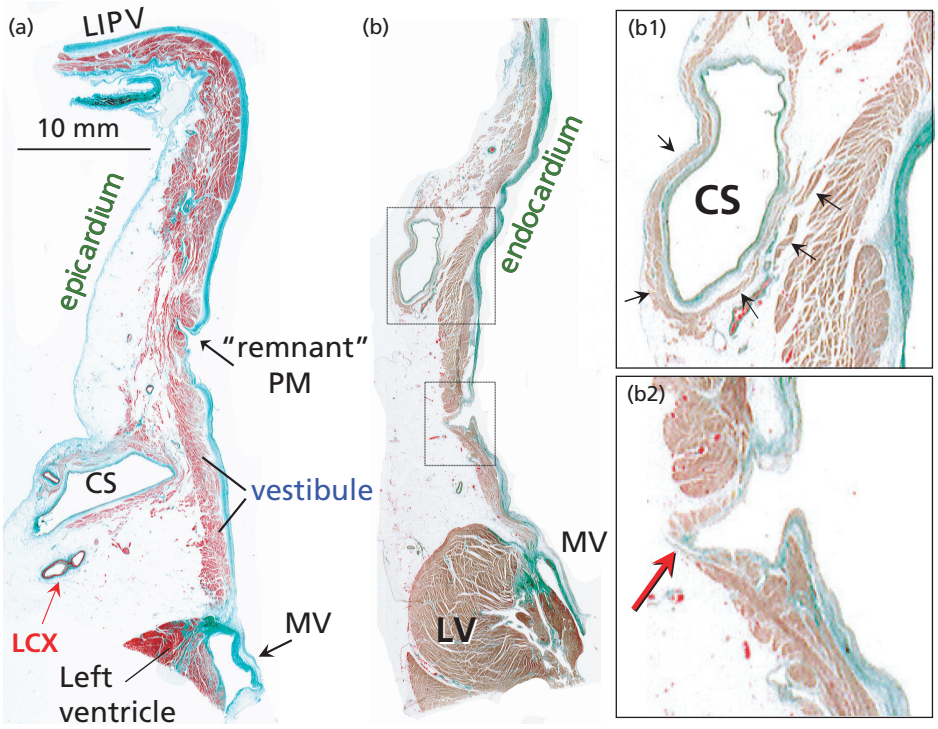

Figure 1.15 (a, b) Longitudinal sections at the mitral isthmus to illustrate its anatomic relations with the coronary sinus (CS) and circumflex artery (LCX). (b) The coronary sinus is surrounded by a sleeve of muscle from the left atrial wall (arrows in b1). Note in (b2) the space between the pectinate muscles where the left posterior atrial wall becomes thinner (red arrow). Note also the distance of the coronary sinus to the hingeline of the mitral valve. (Trichrome stain.) LIPV, left inferior pulmonary vein; LV, left ventricle; MV, mitral valve.

isthmus. The study by Becker showed that the mean myocardial thickness of the mitral isthmus at the level of the PV orifice was 3.0 mm (range 1.4–7.7 mm). The thickness midway in between the PV and the mitral annulus was 2.8 mm (range 1.2–4.4 mm) and that at the mitral valve annulus was 1.2 mm (range 0–3.2 mm) [85]. By contrast, a recent histological examination revealed that the thickest atrial wall was midway between the mitral annulus and the left inferior PV with tapering at either end of the isthmus [86]. Wittkampf et al. have suggested that the muscle sleeve around the coronary sinus and the close anatomic proximity of the circumflex artery are the two major anatomic determinants for the creation of mitral isthmus conduction block [86]. Atrial arteries fully embedded in atrial myocardium closer than 5 mm from the endocardium are likely to be damaged by transmural lesions. In addition, local cooling mediated by atrial arteries and veins may protect the surrounding left atrial myocardium, preventing the formation of transmural lesions by radiofrequency current applications, thus making it difficult or impossible for the creation of conduction block through the mitral isthmus. Also relevant is the presence of small crevices close to the base of the LAA that may entrap the tip of the ablation catheter, increasing the risk of isthmus perforation [86] (Figure 1.15).

During the ablation procedure, the position of the catheter introduced in the coronary sinus is used as an anatomic marker of the mitral annulus. However, previous anatomic studies showed that the great cardiac vein is not a good landmark to spot the mitral annulus [85,86]. This venous structure runs on the atrial side of the left atrioventricular groove at a considerable distance from the mitral annulus (6 mm in the most distal sector of the great cardiac vein, and up to 11 mm in the most proximal portion close to the ostium of the coronary sinus).

Architecture of the PV–atrial junction and left posterior atrial wall: relevance to atrial fibrillation ablation

Muscular myoarchitecture of the venoatrial junction and pulmonary veins

The presence of atrial myocardial tissue extending over the wall of the PVs has been confirmed both macroscopically and histologically by many investigators (Figure 1.16). The studies of Burch and Romey [87] and Nathan and Eliakim (88) in the mid 20th century drew attention to the potential function of these muscular sleeves. At that time, the role of myocardial sleeves in the pulmonary veins was thought to be that of a sphincter capable of acting like a "throttle valve" and causing pulmonary edema. It is also recognized that the PVs are capable of generating electrical impulses independently [89–91]. The venous wall in humans shows an innermost layer wall formed by a thin endothelium overlying an irregular media of connective tissue and smooth muscle cells, and a thick outer layer of fibrous adventitia. At the PV–atrial junction, the endocardium of the LA is in continuity with the

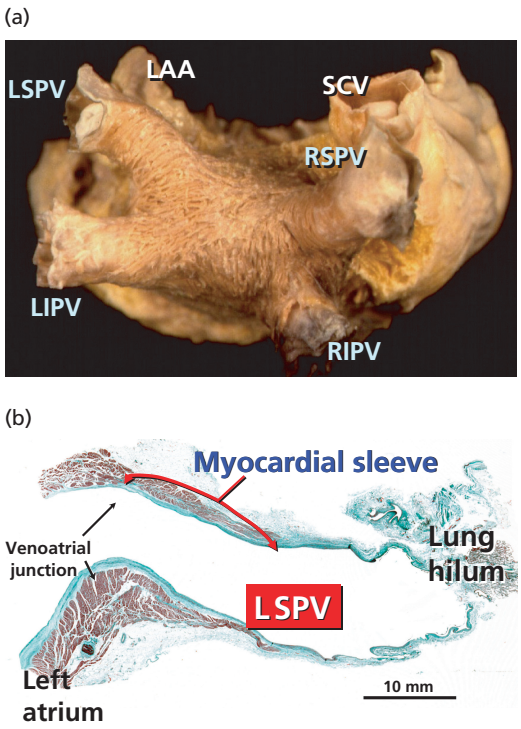

Figure 1.16 (a) Arrangement of the subepicardial myofibers around the pulmonary venous orifices. The myocardial tissue encircles the venoatrial junction forming the myocardial sleeve. The right superior pulmonary vein (RSPV) lies immediately behind the superior caval vein (SCV). (b) Histological longitudinal sections through a left superior pulmonary vein (LSPV). The myocardial sleeve extends over the wall of the PV from the LA. The sleeve are thicker at the venoatrial junction and thinner towards the lung hilum. LAA, left atrial appendage; LIPV, left inferior pulmonary vein; RIPV, right inferior pulmonary vein.

endothelial lining of the vein. The transition from the venous media to the left atrial subendocardial region is represented by a gradual decline in the number of smooth muscle cells. In most PVs (96%) the smooth muscle of the venous wall overlaps with a layer of myocardial bundles extending over the inner layer but is separated from it by a thin plane of fibro-fatty tissue. This intermediate myocardial layer, between the adventitia and the venous media, is the myocardial continuity from the left atrial wall (so-called myocardial sleeves) in a fine matrix composed of collagen, elastic fibers, and blood vessels [41,42]. Therefore, as seen in longitudinal sections, the extension of the left atrial musculature lies external to the venous wall and within the epicardium/adventitia.

In our histological study on 65 veins [42], the thickness of the smooth muscle ranged from 0.05 to 1 mm at the venoatrial junction, diminishing to 0.03–0.5 mm at a distance of 10 mm from the junction. The lengths of the sleeves varied from vein to vein, and the distal margins were irregular in most of the specimens, especially those of the inferior veins which tended to have less myocardial coverage than the superior veins. In keeping with previous anatomic studies, the sleeves in the superior right and left PVs were longer than those observed in the inferior veins. The sleeves were thickest at the venoatrial junction (1.88 ± 0.45 mm, range 1.2–2.8 mm) and then tapered toward the lung hilums, but the decrease in thickness was not uniform circumferentially. The atrial myocardial sleeves in the superior veins were thickest inferiorly (at 6 o'clock), and thinnest superiorly (at 12 o'clock), whereas an opposite pattern was found in the inferior veins. When superior and inferior veins were compared, the sleeves were thickest in the left superior veins. The mean thickness of adventitia and endocardium/venous wall also decreased from the venoatrial junction toward the lungs. Electrophysiological studies using a circular multielectrode catheter to obtain a circumferential mapping of the PVs demonstrated a non-homogeneous pattern of PV activation and revealed the presence of critical sites of atriovenous connection that enable us to achieve the electrical isolation of the PV without a circumferential ablation. Ablation confirms that these critical sites of myocardial venoatrial connection are most often located at the bottom of the superior PVs (85% of the cases) and at the top of inferior PVs (75% of the cases) [92].

The anatomic orientation of the myocardial fibers making up the sleeves is highly variable. Although the sleeves are mainly composed of circularly orientated bundles, oblique and longitudinally oriented fibers are also common [41,93]. These architectural observations are consistent with mapping studies of the PVs in the living human heart, demonstrating conduction patterns in a longitudinal and transverse direction [94]. A longitudinal pattern of activation is a strong predictor of ostial sites that require the application of ablative energy to electrically isolate the PV, whereas those with a transverse activation pattern are much less likely to require ablation. Recent electrophysiological studies in humans have demonstrated the presence of electrical conduction between the upper and lower left PVs, which may imply isolation of contiguous vessels from a single or circumscribed region to achieve complete PV electrical disconnection [95,96]. At the level of the venoatrial junction, we found in our specimens myocardial fibers crossing the isthmus between the superior and inferior venous orifices in both right and left PVs (Figure 1.17). These crossing fibers were found in 41% of the hearts at the level of the left PVs, and in the right PVs in 25% of hearts. Histological examinations showed that the myocardial fibers connecting the two contiguous PVs run along the posterior wall of the superior PVs and cross through the interpulmonary isthmus to the anterior margin of the inferior PV in 63% of hearts, whereas a reverse orientation (from anterior to posterior PV wall) was observed in another 37% of the connecting veins. The histological thickness of the crossing fibers showed variations in the maximal thickness at the venoatrial junctions ranging from 0.2 to 2.5 mm. The prevalence of muscular connections between the veins at the level of the venoatrial junction was independent of the distance between the orifices of the right and left PVs.

At the venoatrial junction, gaps of myocardial tissue of irregular morphology and small areas of myocardial degeneration with fibrous replacement can be found in 34% of the veins across the age range of the people from whom the specimens

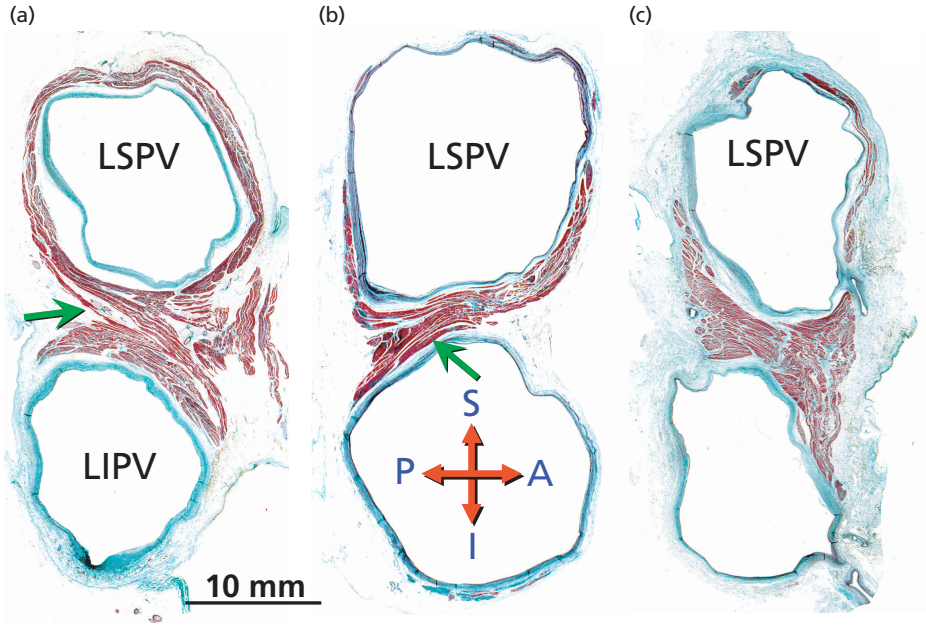

Figure 1.17 Histological cross-sections through three sets of left pulmonary veins (PVs) showing the variation in circumferential arrangement and thickness of the myocardial sleeves (a, b, c). The myocardial thickness varied from vein to vein and the sleeves are thicker in the area close to adjacent veins. The inferior veins have less myocardial coverage than the superior veins. (a, b) Myocardial fibers (green arrows) crossing the isthmus between the orifices of the left superior PV (LSPV) and left inferior PV (LIPV). (a) The fibers runs along the posterior wall of the superior PV crossing through the interpulmonary region to the anterior margin of the inferior PV; (b) a reverse orientation of the muscular connections.

were obtained [41] (Figure 1.18). The presence of collagenous septa between myocardial fibers may result in progressive electrical uncoupling of the side-to-side connections between groups of parallel atrial fibers. These findings are important, since they may be the basis for a non-uniform anisotropic conduction of a wavefront at a given area and for the development of reentry within smaller regions [97–99]. A recent postmortem morphological study found a higher incidence of myocardial sleeves with more severe discontinuity, hypertrophy, and fibrosis in patients with AF than in those without the latter arrhythmia [100]. Hocini et al. [101] correlated the conduction properties with the anatomic myofiber architecture of the canine pulmonary veins and showed zones of activation delay correlating with histological assessment of myofiber arrangement and distribution with sudden change in myocardial fiber orientation. These findings suggest that micro reentry could occur or promote the exit of activation from a focal source. In our series of structurally normal human hearts, we did not observe node-like cells or discrete tract of specialized myocites as found by other studies in animals [102] and humans [103].

Muscular myoarchitecture of the left posterior atrial wall

It is still unclear whether the initiation and maintenance of human AF depends on automatic focal or reentrant mechanisms. Initial catheter ablation approaches were aimed at obtaining an electrical disconnection of the PVs so as to isolate the LA from the venous triggers. Additional linear lesions targeting the region of the posterior left atrial wall have been shown to increase the success rate of catheter ablation in paroxysmal, persistent, and chronic AF. Recent reports have shown the contribution of different atrial regions on the fibrillatory process and to the maintenance of AF, emphasizing the role of structural discontinuities and heterogeneous fiber orientation favoring anatomic reentry or anchoring rotors [17–23]. Modification of the

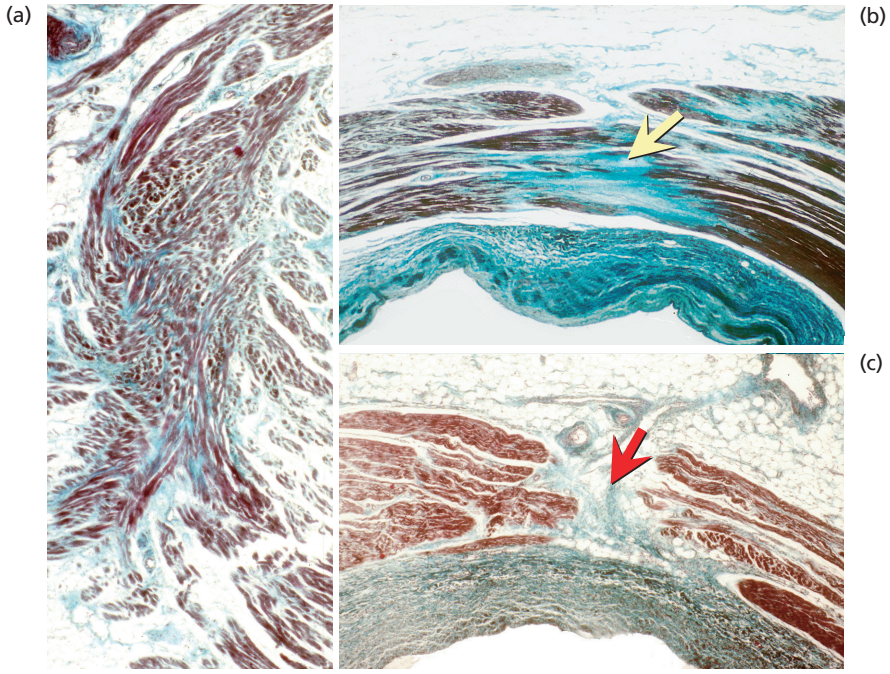

Figure 1.18 (a) Histological longitudinal section of the myocardial sleeve of the right superior PV at the venoatrial junction. Note the mixed arrangement of myocardial fibers making up the myocardial sleeves. (b, c) Cross-sections illustrating a small area of myocardial degeneration with fibrous replacement (yellow arrow, b) and the presence of gaps of connective tissue bridges between the myocardial fibers (red arrow, c)

atrial substrate by targeting structures of the LA that are thought to maintain AF appears to increase success rates. The posterior wall of the LA, for example, seems to play an important role in maintaining AF. Morillo et al. reported in a canine model of AF that cryoablation at sites of short cycle length activity in the posterior LA resulted in the interruption of this arrhythmia [104]. Observations from the laboratory of Jalife and co-workers [105–107] demonstrated in the isolated sheep heart the presence of a small number of stable ongoing circuits generating high frequency waves and providing a base to generate fibrillatory conduction. Data derived from high resolution optical mapping in this animal model also showed that the focal sources correspond to single or a small number of reentrant rotors discharging at a high frequency and that these are localized in the PV orifices or at the contiguous posterior left atrial region. Postmortem examination in human specimens, showed in most hearts an abrupt change of subendocardial fiber orientation (circumferential, oblique, and longitudinal) in the posterior wall of the LA at the venoatrial junctions (Figure 1.19). In these areas the subendocardial fibers are usually loop-like extensions from the longitudinal fibers encircling the venoatrial junctions [40]. Also relevant is the finding of changes in myoarchitecture transmurally. Histology confirmed the changes in fiber orientation in the subendocardium and also revealed crossover arrangements deeper in the wall. The most obvious broad band or linear anatomic barrier of longitudinal and oblique fibers was formed by the "septopulmonary bundle" that also marked a change in LA wall thickness. This was thicker toward the septum (1.4 ± 0.5 mm) and thinner laterally (0.7 ± 0.4 mm). Left atrial endocardial activation was mapped in 19 patients with a percutaneous non-contact mapping system during episodes of focal initiation of AF [108]. In this study Markides et al. observed that the pattern of LA activation was predominantly determined by a principal line of conduction block [108]. It appears to be related to the linear anatomic barrier identified by the examination of fiber orientation. Another area of change in subendocardial fiber orientation was observed adjacent to the anterior mitral valve annulus in seven of 10 hearts, whereas abundant

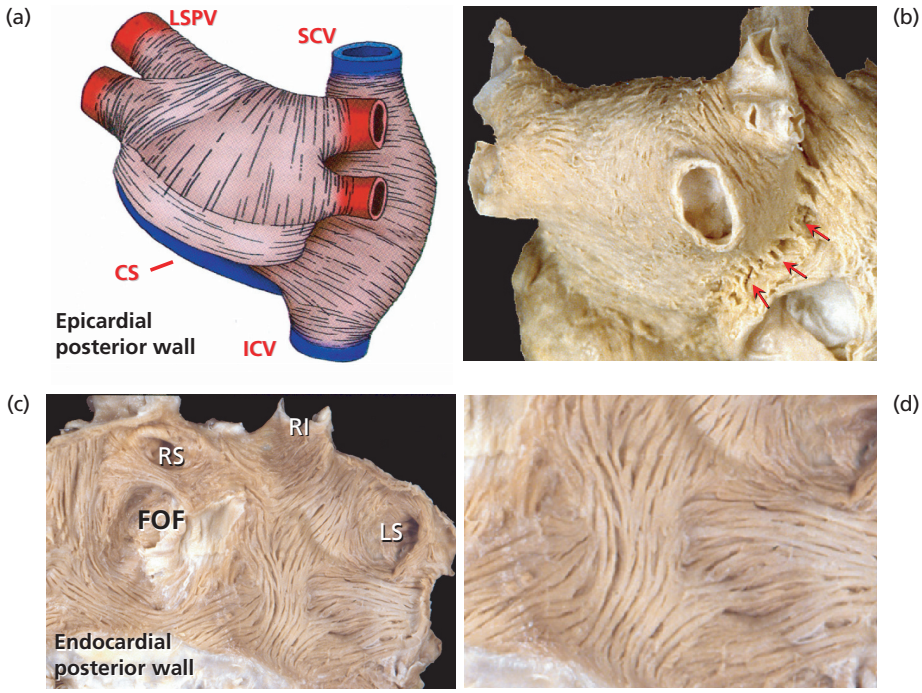

Figure 1.19 Schematic representation of the general arrangement of myocardial fibers (a) and subepicardial dissection seen from the postero-epicardial aspect (b). Note in (b) the interatrial muscular bridges (arrows) crossing the septal raphe. (c, d) Dissection of the subendocardium showing the abrupt change of subendocardial fiber orientation in the posterior region of the LA. (d) Enlarged figure showing the predominantly longitudinal orientation of the myocardial fibers of the posterior left atrial wall encircling the orifice of the PV subendocardially. CS, coronary sinus inferior; FOF, flap oval fossa; ICV, inferior caval vein; LS, left superior pulmonary vein; LSPV, left superior pulmonary vein; RI, right inferior pulmonary vein; RS, right superior pulmonary vein; SCV, superior caval vein.

fatty tissue was observed above the posterior mitral valve annulus in six of 10 hearts [108].

The coronary sinus

The topic of early recurrence of AF after catheter ablation is far from being settled. It has been said that early recurrence is due to recovery of conduction of previously isolated PVs and in some cases to the existence of non-PV foci that were not properly identified at the initial ablation session. Non-PV foci can be located at the posterior LA wall close to the orifices of the PVs or be related to non-pulmonary thoracic veins such as caval veins, the oblique vein of Marshall, or the musculature lining of the coronary sinus [27–32].

The coronary sinus runs along the inferior aspect of the LA and opens into the right atrium through an ostium. The oblique vein of Marshall and the valve of Vieussens (found in 87% of patients) can been used as anatomic landmarks to define the distal limits of the coronary sinus from the ostium of the coronary venous system [109] (see Figure 1.13). The inferior portion of the vestibular component of the LA (smooth circumferential area surrounding the orifice of the mitral valve) directly apposes the wall of the coronary sinus. Here, posteriorly and parietally, the atrial wall is thin and overlies the great cardiac vein. The coronary sinus, and its continuation into the great cardiac vein, has it own muscular wall that increases in thickness the closer it is to its ostium in the right atrium. These muscular sleeves extend from the ostium to 25–52 mm distally along the wall of the coronary sinus [109]. Frequently, small tongues of myocardial fibers extend from the coronary sinus to insert into the posterior and inferior wall of the left atrium (Figure 1.19).

Electrophysiological studies have also demonstrated the electrical connection between the right atrium and LA through the musculature of the coronary sinus [110,111]. Recent observations have identified focal sources of premature depolarizations originating within the coronary sinus that may trigger AF [29]. It has been suggested that electrical

disconnection of the two atria targeting the interatrial connections diminishes the electrophysiological substrate for perpetuation of AF [29,112].

The esophagus and other extracardiac structures

As repeatedly stated, catheter ablation techniques in patients with AF have progressively evolved to more extensive procedures. Two of the most widely used approaches involve not only circumferential ablation around the PVs but also the performance of linear lesions between the encircled PV orifices and between the left lower PV and the mitral annulus. These linear lesions involve the posterior wall of the LA. In addition, catheter ablation tools capable of creating larger and deeper lesions are increasingly used to reduce the number of pulses and the duration of the procedure and to assure transmurality of the ablation. The current approaches creating linear lesions on the posterior LA wall, in combination with tools capable of generating deeper lesions, has resulted in new, albeit rare, complications for catheter ablation of AF: atrioesophageal fistula, vagal injury resulting in gastric hypomotility, and phrenic nerve injury resulting in diaphragmatic paralysis [34–36].

Morphological relation between the esophagus and posterior left atrial wall

The development of an atrioesophageal fistula after catheter ablation in the posterior wall of the LA is probably the most severe complication that has been encountered in patients subjected to an ablation procedure. Understanding the spatial relations between the esophagus and the LA is essential to reduce risk.

The esophagus descends in virtual contact with the posterior LA. In its upper course, the esophagus is situated slightly to the left between the trachea and the vertebral column (see Figure 1.7). It then passes behind the LA and to the right of the aortic arch to descend to the posterior mediastinum along the right side of the descending thoracic aorta. In a recent anatomic study we examined the course of the esophagus in 15 cadavers [52]. The length of the esophagus in contact with the posterior LA ranged between 30 and 53 mm (mean 42 ± 7 mm). Transversely, the width of the esophagus in contact with the posterior LA wall was 13. ± 5 mm (range 9–15.5 mm) (Figures 1.20 and 1.21). It is important to recognize that the esophagus follows a variable course along the posterior aspect of the LA. It was < 5 mm from the endocardium in 40% of specimens. In 40% of cases it passed along the middle portion of the posterior LA wall (Figure 1.20). In 20% of specimens it descended close to the right venoatrial junction; in the remaining cases it had a leftward course close to the left venoatrial junction [52]. However, the esophagus coursed obliquely from left superior to right inferior in 36% of patients, and can move during the ablation procedure from one side to the other [113]. Being able to image the esophagus during the procedure can reduce the risk of damaging it.

Behind the posterior left atrial wall is a layer of fibrous pericardium and fibro-fatty tissue of irregular thickness that contains esophageal arteries and

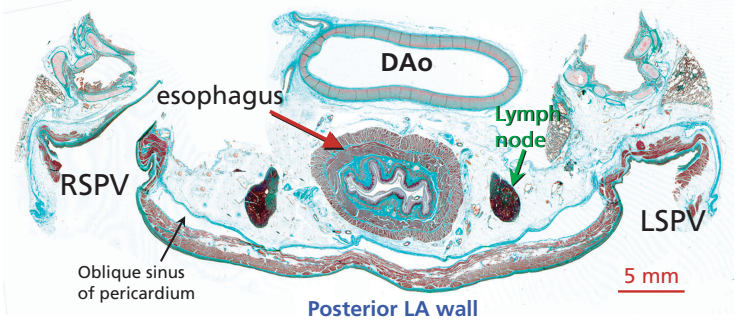

Figure 1.20 Transverse histological sections (Masson's trichrome stain) showing the proximity of the esophagus to the middle of the posterior wall of the left atrium (LA). DAo, descending aorta; LSPV, left superior pulmonary vein; RSPV, right superior pulmonary vein.

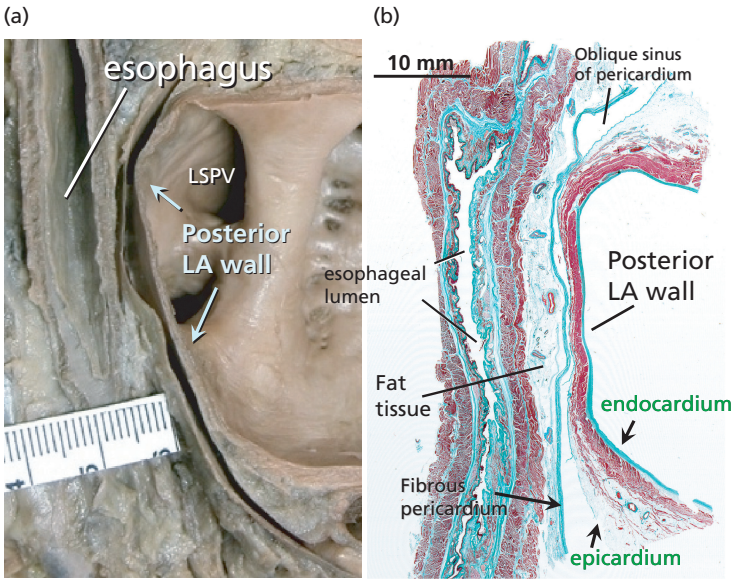

Figure 1.21 (a) Sagittal section through the left atrium (LA) and esophagus showing how the esophagus is related to the middle of the posterior wall of the LA. (b) Histological section (Masson's trichrome stain) in similar orientation showing the fibrous pericardium between the posterior left atrial wall and the esophageal wall and the fatty tissue plane immediately behind that. LSPV, left superior pulmonary vein.

the vagus nerve plexus (Figures 1.20–1.22). These anatomic structures may be affected by ablative procedures. It has been shown that radiofrequency may substantially elevate the temperature within the esophageal lumen and that atrioesophageal fistulae may result from this thermal injury. The heat from the probe may also result in subacute inflammatory reaction of the esophageal wall. Overlapping lines in the posterior wall may have been responsible for esophageal injury. Thus, the investigators recommend avoiding excessively deep lesions by decreasing the power, temperature, and duration of radiofrequency energy application. The posterior left atrial wall is significantly thinner at the superior part of the LA (2.2 ± 0.5 mm in the left venoatrial junction) [52] (Figure 1.21). The esophagus is not in direct contact with the roof of the LA, thus some investigators also suggest that the posterior ablation line should be placed at the LA roof to avoid esophageal injury.

Anatomic risk of phrenic nerve injury

A few instances of phrenic nerve injury have been reported after catheter ablation. The incidence of this complication seems to depend on the type of ablation source: 0.1% using radiofrequency energy, 0.6% utilizing cryothermal ablation, 6% with ultrasound approaches, and 5% using laser energy [37,38]. The right phrenic nerve has a close anatomic relationship with the superior caval vein (minimum distance 0.3 ± 0.5 mm) and the right superior pulmonary vein (minimum distance 2.1 ± 0.4 mm) as it runs through the lateral and posterolateral wall of the right atrium [114,115] (Figure 1.23). In 32% of our unselected human heart specimens the anterior wall of the right superior PV was < 2 mm from the right phrenic nerve [115]. Consequently, catheter ablation techniques aimed at modifying the sinus node function at the lateral right atrium and catheter ablation for AF at the orifice and adjacent area of the right superior PV carry a certain risk of injuring the right phrenic nerve [37].

On the other hand, the left phrenic nerve is in the vicinity of the lateral vein of the heart, the great cardiac vein, the left atrial appendage, and the lateral wall of the left ventricle. We observed that the left phrenic nerve passed over the left atrial appendage and descended along the obtuse cardiac margin in relation with the left obtuse marginal vein (minimum distance 3.5 ± 0.5 mm) in 79% of our specimens (Figure 1.24). In the remaining specimens, its course was anterosuperior, passing over the main

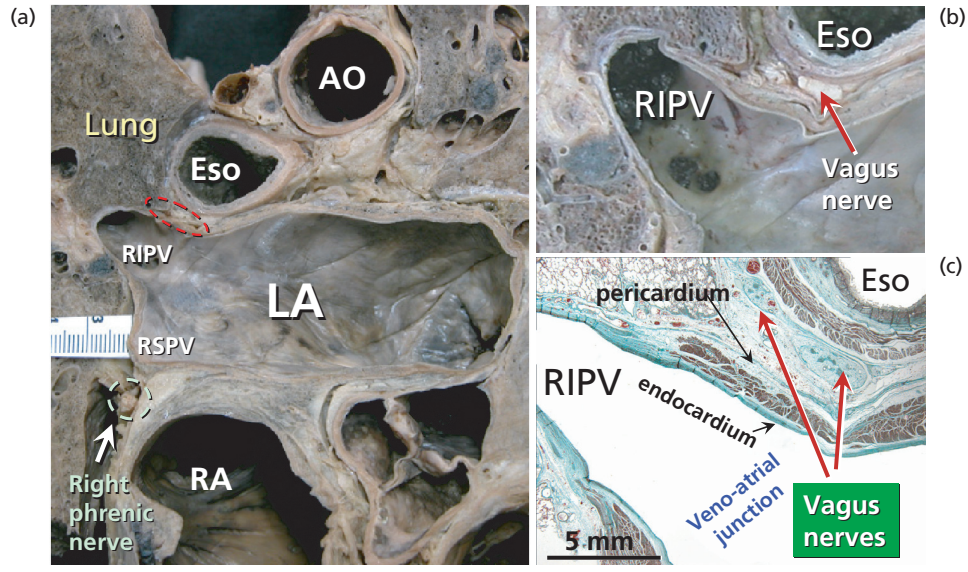

Figure 1.22 An overview of a transthoracic section through the mediastinum showing the locations of the vagus nerves (red dashed circle) and the phrenic nerve (green dashed circle) relative to the PVs and left atrium (LA). (b) A close-up of the right inferior venoatrial junction. (c) A corresponding histological section (trichrome stain). AO, aorta; Eso, esophagus; RA, right atrium; RIPV, right inferior pulmonar vein; RSPV, right superior pulmonary vein.

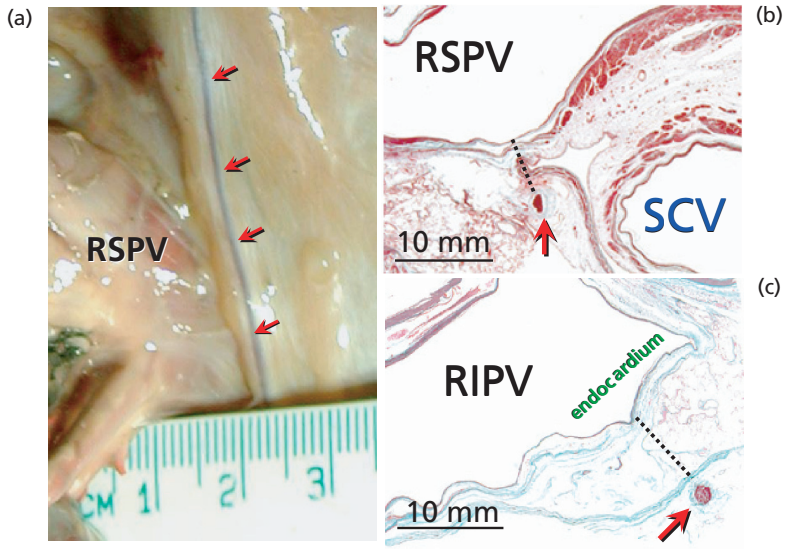

Figure 1.23 (a) Dissection of the right superior pulmonary vein (RSPV) close to the right phrenic nerve (red arrows). (b, c) Histological sections through the RSPV and right inferior pulmonary vein (RIPV), respectively. The right phrenic nerve (red arrows) is adherent to the fibrous pericardium (stained green). The broken lines indicate the distance between the endocardium of the right PVs and the right phrenic nerve. (Masson's trichrome stain.) SCV, superior caval vein.

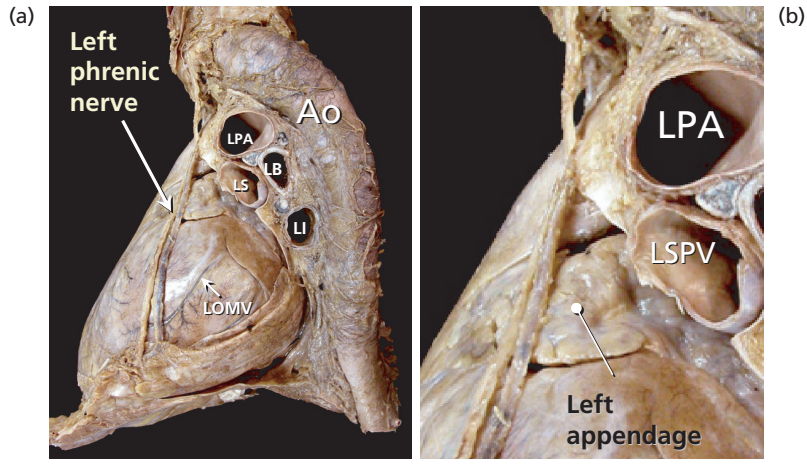

Figure 1.24 (a, b) Left lateral view of the heart showing the close anatomic relation of the left phrenic nerve with the LAA and the left obtuse marginal vein (LOMV). Ao, aorta; LB, left bronchus; LI, left inferior pulmonary vein; LPA, left pulmonary artery; LS, left superior pulmonary vein; LSPV, left superior pulmonary vein.

stem of the left coronary artery or the anterior descending artery and the great cardiac vein (minimum distance 1.4 ± 0.3 mm). Catheter ablation or pacing close to these areas may cause injury of the left phrenic nerve [116]. In the human clinical setting, transient phrenic nerve paresis has been observed during cryoablation of the right superior pulmonary vein in 2% of patients [117]; others [116] have reported functional recovery from phrenic nerve injury, although two of 17 patients developed pulmonary complications, with one needing a recovery period of up to 28 months. Recurrent pneumonia and dependence on mechanical ventilation are serious complications that can lead to a vicious circle.

Anatomic relations between the left atrium and the neighboring vagus nerves

Thermal injury may involve the periesophageal vagal nerves, resulting in acute pyloric spasm and gastric hypomotility [39]. The vagus nerves pass behind the root of the lungs and form the right and left posterior pulmonary plexuses [40]. From the caudal part of the left pulmonary plexus two branches descend on the anterior surface of the esophagus, joining with a branch from the right pulmonary plexus to form the anterior esophageal plexus. The anterior esophageal plexus passes external to the pericardial sac but in very close proximity to the posterior and the right and left venoatrial junctions (Figure 1.25). The posterior and anterior esophageal plexuses enter the abdomen through the diaphragm to become the posterior and anterior vagal trunks that innervate the pyloric sphincter and the gastric antrum. Shah et al. [39] recently reported four patients who underwent ablation of the ostial PVs and posterior LA who experienced an acute delayed gastric emptying syndrome 3–48 h after the procedure. Our observation on seven normal cadavers revealed a mean distance between the bundles of the anterior esophageal plexus and the posterior left atrial endocardium of 4.1 ± 1.4 mm (range 2.5–6.5 mm) [118] (see Figure 1.22).

Left atrial autonomic nervous system content

Experimental studies have shown that initiation and maintenance of AF can be enhanced by both parasympathetic and sympathetic stimulation [119–127]. Elvan et al. [120] in an animal model of AF by atrial and cervical vagal stimulation abolished induction of sustained AF by circumferential ablation of the PVs. Schauerte et al. [122] also demonstrated in dogs that selective vagal denervation along the right pulmonary artery prevents vagal-induced AF. In patients with AF, Pappone et al. [24] have shown that complete vein denervation is an additional predictor of long-term benefit

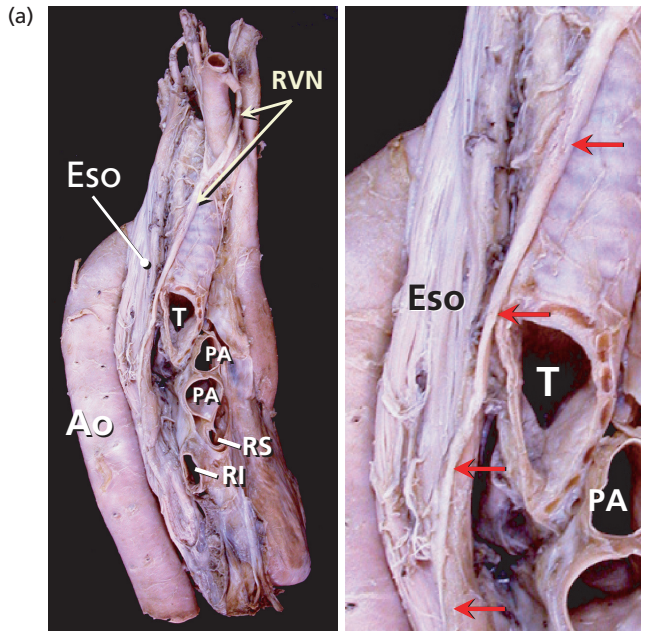

Figure 1.25 (a) Posterior view of the esophagus (Eso), descending thoracic aorta (Ao), and trachea (T) to show the course of the esophagus and its relationship with the right vagus nerve (RVN). (b) Enlarged figure with the right vagus nerve indicated (red arrows). PA, pulmonary artery; RI, right inferior pulmonary vein; RS, right superior pulmonary vein.

after circumferential PV ablation of AF. More recently, Scanavacca et al. [25] have demonstrated that catheter ablation of selected atrial sites where high frequency stimulation induced vagal reflexes, may prevent AF recurrence in patients with vagal-induced paroxysmal AF. The above studies represent an additional piece of the complex and still unassembled puzzle that is the pathophysiology of AF, and reinforce the need of revisiting the anatomy of the autonomic nervous system elements of the LA.

Abundant nerves and ganglions of the autonomic nervous system are present at the junction between the PVs and the LA, and some more distally inside the vein. A regional distribution of the cardiac nerves and differential patterns of innervation have been observed in mammalian hearts. In the human LA, ganglionated plexuses were observed in the superior surface between the PVs and in the posterior aspect of the LA. Preganglionic parasympathetic fibers and postganglionic sympathetic fibers come together in the fat pads on the epicardial surface of the posterior LA wall [123]. Histochemical studies for acetylcholinesterase have shown epicardial ganglionated nerves that extend through three neural pathways or subplexuses in the LA: the left ventral, left dorsal, and middle dorsal. Interestingly the left dorsal subplexus extends over the area of the vein of Marshall along the epicardial aspect of the left posterolateral ridge [124].

Chiou et al. [125] showed that transmural lesions were needed to denervate the atria, and it was felt that the autonomic nervous system elements were mainly present subepicardially rather than endocardially. However, the presence of innervation within the myocardium of the LA suggests that non-transmural lesions may have an impact on atrial innervation. A quantitative histological evaluation identified gradients of innervation in the LA and in the PVs [126]. This study showed that the greatest nerve densities were found in the left and posterior parts of the LA and at the antrum of the PVs. Left-sided PVs had a more dense content of nervous system elements than the right-sided veins, and the density of innervation was higher at the orifices of the PVs than in their distal segments. In a recent immunohistochemical study, Tan et al. [127] have demonstrated that adrenergic and cholinergic nerve densities are highest within 5 mm of the junction between the PVs and the LA and that because both sympathetic and parasympathetic elements are highly co-located, it is impossible to define areas for a selective vagal or sympathetic ablation.

Conclusion

In one and a half decades catheter ablation has been shown to be an increasingly important therapeutic option for patients with paroxysmal, persistent, and chronic atrial fibrillation. Ablation techniques have evolved from rather limited initial approaches to quite extensive atrial interventions. In spite of more or less substantial differences among the various techniques that are currently utilized worldwide, results seem to be uniformly similar with success rates in the range of 70–90%. Because the amount of myocardium that is ablated at the present time is more extensive, the rate and type of complications of ablation in AF might also be larger. The time has come to ascertain if some of these approaches are unnecessarily extensive. We are far from being able to answer this question but we believe that the refinement and tuning of catheter ablation techniques for atrial fibrillation has to come from a better understanding of the anatomo-functional substrate of the arrhythmia. In this chapter we have reviewed the gross morphological details of the PV orifices and their neighboring left atrial landmarks and the myocardial architecture of the venoatrial junction and the posterior atrial wall. In addition, we described the anatomy and architecture of the left atrial appendage, the left posterolateral ridge, the vein of Marshall, and the coronary sinus. Finally, the autonomic innervation of the atria, as well as the relations between the left atrium and the pulmonary veins with the extracardiac structures, are also described.

References

1 Jais P, Haissaguerre M, Shah DC, et al. A focal source of atrial fibrillation treated by discrete radiofrequency ablation. *Circulation* 1997;**95**:572–6.

2 Haïssaguerre M, Jais P, Shah DC, et al. Spontaneous initiation of atrial fibrillation by ectopic beats originating in the pulmonary veins. *N Engl J Med* 1998;**339**: 659–66.

3 Chen SA, Hsieh MH, Tai CT et al. Initiation of atrial fibrillation by ectopic beats originating from the pulmonary veins: electrophysiological characteristics, pharmacologic responses and effects of radiofrequency ablation. *Circulation* 1999;**100**:1879–86.

4 Haissaguerre M, Jais P, Shah DC, et al. Catheter ablation of chronic atrial fibrillation targeting the reinitiating triggers. *J Cardiovasc Electrophysiol* 2000;**11**:2–10.

5 Chen SA, Tai CT, Tsai CF, et al. Radiofrequency catheter ablation of atrial fibrillation initiated by pulmonary vein ectopic beats. *J Cardiovasc Electrophysiol* 2000;**11**:218–27.

6 Haissaguerre M, Shah DC, Jais P, et al. Electrophysiological breakthroughs from the left atrium to the pulmonary veins. *Circulation* 2000;**102**:2463–5.

7 Haissaguerre M, Jais P, Shah DC, et al. Electrophysiological end point for catheter ablation of atrial fibrillation initiated from multiple pulmonary venous foci. *Circulation* 2000;**101**:1409–17.

8 Oral H, Knight BP, Tada H, et al. Pulmonary vein isolation for paroxysmal and persistent atrial fibrillation. *Circulation* 2002;**105**:1077–81.

9 Ernst S, Schluter M, Ouyang F, et al. Modification of the substrate for maintenance of idiopathic human atrial fibrillation: efficacy of radiofrequency ablation using nonfluoroscopic catheter guidance. *Circulation* 1999; **100**:2085–92.

10 Pappone C, Rosanio S, Oreto G, et al. Circumferential radiofrequency ablation of pulmonary vein ostia. *Circulation* 2000;**102**:2619–28.

11 Pappone C, Oreto G, Rosanio S, et al. Atrial electroanatomic remodeling after circumferential radiofrequency pulmonary vein ablation: efficacy of an anatomic approach in a large cohort of patients with atrial fibrillation. *Circulation* 2001;**104**(21):2539–44.

12 Oral H, Sharf C, Chugh A, et al. Catheter ablation for paroxysmal atrial fibrillation. Segmental pulmonary vein ostial ablation versus left atrial ablation. *Circulation* 2003;**108**:2355–60.

13 Jais P, Hocini M, Sanders P, et al. Technique and results of linear ablation at the mitral isthmus. *Circulation* 2004;**110**:2996–3002.

14 Ernst S, Ouyan F, Lober F, et al. Catheter-induced linear lesions in the left atrium in patients with atrial fibrillation: an electroanatomic study. *J Am Coll Cardiol* 2003;**42**:1271–82.

15 Ouyang F, Bansch D, Ernst S, et al. Complete isolation of left atrium surrounding the pulmonary veins. New insights from the double-lasso technique in paroxysmal atrial fibrillation. *Circulation* 2004;**110**:2090–6.

16 Jais P, Haisaguerre M, Shah DC, et al. Regional disparities of endocardial atrial activation in paroxysmal atrial fibrillation. *Pacing Clin Electrophysiol* 1996;**19**:1998–2003.

17 Todd DM, Skanes AC, Guiraudon G, et al. Role of the posterior left atrium and pulmonary veins in human lone atrial fibrillation: electrophysiological and pathological data from patients undergoing atrial fibrillation surgery. *Circulation* 2003;**108**:3108–14.

18 Nademanee K, McKenzie J, Kosar E, et al. A new approach for catheter ablation of atrial fibrillation:

mapping of the electrophysiological substrate. *J Am Coll Cardiol* 2004;**43**:2044–53.

19 Haissaguerre M, Sanders P, Hocini M, et al. Catheter ablation of long-lasting persistent atrial fibrillation: critical structures for termination. *J Cardiovasc Electrophysiol* 2005;**16**:1125–37.

20 Sanders P, Berenfeld O, Hocini M, et al. Spectral analysis identifies sites of high frequency activity maintaining atrial fibrillation in humans. *Circulation* 2005;**112**: 789–97.

21 Haissaguerre M, Hocini M, Sanders P, et al. Localized fibrillatory sources maintaining atrial fibrillation. *Heart Rhythm* 2005;**2**:S20.

22 Rostock T, Rotter M, Sanders P, et al. Fibrillating areas isolated within the left atrium after radiofrequency liner catheter ablation. *J Cardiovasc Electrophysiol* 2006;**17**: 1–6.

23 Haisaguerre M, Hocini M, Sanders P, et al. Localized sources maintaining atrial fibrillation organized by prior ablation. *Circulation* 2006;**113**:616–25.

24 Pappone C, Santinelli V, Manguso F, et al. Pulmonary vein denervation enhances long-term benefit after circumferential ablation for paroxysmal atrial fibrillation. *Circulation* 2004;**109**:327–34.

25 Scanavacca M, Pisani C, Hachul D, et al. Selective atrial vagal denervation guided by evoked vagal reflex to treat patients with paroxysmal atrial fibrillation. *Circulation* 2006;**114**:876–85.

26 Jais P, Shah DC, Haisaguerre M, et al. Efficacy and safety of septal and left-atrial linear ablation for atrial fibrillation. *Am J Cardiol* 1999;**84**:139R–146R.

27 Chen PS, Wu TJ, Hwang C, et al. Thoracic veins and the mechanism on non-paroxysmal atrial fibrillation. *Cardiovas Res* 2002;**54**:295–301.

28 Tsai CF, Tai CT, Hsieh MH, et al. Initiation of atrial fibrillation by ectopic beats originating from the superior vena cava: electrophysiological characteristic and results of radiofrequency ablation. *Circulation* 2000; **102**:67–74.

29 Oral H, Ozaydin M, Chugh A, et al. Role of the coronary sinus in maintenance of atrial fibrillation. *Cardiovasc Electrophysiol* 2003;**14**:1329–36.

30 Hwang C, Wu TJ, Doshi RN, et al. Vein of Marshall cannulation for the analysis of electrical activity in patients with focal atrial fibrillation. *Circulation* 2000;**101**: 1503–5.

31 Katritsis D, Ioannidis JPA, Anagnostopoulos CE, et al. Identification and catheter ablation of extracardiac and intracardiac components of ligaments of Marshall tissue for treatment of paroxysmal atrial fibrillation. *J Cardiovasc Electrophysiol* 2001;**12**:750–8.

32 Takahashi Y, Sanders P, Rotter M, et al. Disconnection of the left atrial appendage for elimination of foci maintaining atrial fibrillation. *J Cardiovasc Electrophysiol* 2005;**16**:917–19.

33 Cappato R, Clakins H, Chen SA, et al. Worldwide survey on the methods, efficacy, and safety of catheter ablation for human atrial fibrillation. *Circulation* 2005;**111**: 1100–5.

34 Scanavacca MI, Dávila A, Parga J, et al. Left atrial-esophageal fistula following radiofrequency ablation of atrial fibrillation. *Cardiovasc Electrophysiol* 2004;**15**: 960–2.

35 Pappone C, Oral H, Santinelli V, et al. Atrio-esophageal fistula as a complication of percutaneous transcatheter ablation of atrial fibrillation. *Circulation* 2004;**109**: 2724–6.

36 Cummings JE, Schweikert RA, Saliba W, et al. Brief communication: atrial-esophageal fistulas after radiofrequency ablation. Ann Intern Med 2006;**144**:572–4.

37 Lee BK, Choi KJ, Kim J, et al. Right phrenic nerve injury following electrical disconnection of the right superior pulmonary vein. *Pacing Clin Electrophysiol* 2004;**27**: 1444–6.

38 Sacher F, Monahan K, Thomas S, et al. Phrenic nerve injury after atrial fibrillation catheter ablation. *J Am Coll Cardiol* 2006;**47**:2498–503.

39 Shah D, Dumonceau JM, Burri H, et al. Acute pyloric spasm and gastric hypomotility: an extracardiac adverse effect of percutaneous radiofrequency ablation for atrial fibrillation. *J Am Coll Cardiol* 2005;**46**:327–30.

40 Pai R, Boyle N, Child J, et al. Transient left recurrent laryngeal nerve palsy following catheter ablation of atrial fibrillation. *Heart Rhythm* 2005;**2**:182–4.

41 Ho SY, Sánchez-Quintana D, Cabrera JA, et al. Anatomy of the left atrium: implication for radiofrequency ablation of atrial fibrillation. *J Cardiovasc Electrophysiol* 1999;**10**:1525–33.

42 Ho SY, Cabrera JA, Tran VH, et al. Architecture of the pulmonary veins: relevance to radiofrequency ablation. *Heart* 2001;**86**:265–70.

43 Farré J, Anderson RH, Cabrera JA, et al. Fluoroscopic cardiac anatomy for catheter ablation of tachycardia. *Pacing Clin Electrophysiol* 2002;**25**:79–94.

44 Ho SY, Cabrera JA, Sánchez-Quintana D. Anatomy of the pulmonary vein-atrium junction. In: Chen SA, Haissaguerre M, Zipes D, eds. *Throracic Vein Arrhythmias. Mechanism and Treatment*. Blackwell Futura, Massachusetts, 2004:42–53.

45 Farré J, Cabrera JA, Sánchez-Quintana D, et al. Fluoroscopic and angiographic heart anatomy for catheter mapping and ablation of arrhythmias. In: Huan ST, Wood MA, eds. *Catheter Ablation of Cardiac Arrhythmias*. Saunder Elsevier, Philadelphia, 2006:85–106.

46 Visible Human Slice and Surface Server. Available at http://visiblehuman.epfl.ch.

47 Sánchez-Quintana D, Ho SY, Cabrera JA, et al. Topograhic anatomy of the inferior pyramidal space: relevante to radiofrequency catheter ablation. *J Cardiovasc Electrophysiol* 2001;**2**:210–17.

48 Anderson RH, Webb S, Brown NA. Clinical anatomy of the atrial septum with reference to its developmental components. *Clin Anat* 1999;**12**:362–74.

49 De Ponti R, Zardini M, Storti C, et al. Trans-septal catheterization for radiofrequency catheter ablation of cardiac arrhythmias. Results and safety of a simplified method. *Eur Heart J* 1998;**19**:943–50.

50 Schwinger ME, Tunick PA, Freedberg RS, Kronzon I. Vegetations on endocardial surfaces struck by regurgitant jets: diagnosis by transesophageal echocardiography. *Am Heart J* 1990;**119**:1212–15.

51 Ho SY, Anderson RH, Sánchez-Quintana D. Atrial structure and fibres: morphological basis of atrial conduction. *Cardiovasc Res* 2002;**54**:325–36.

52 Sánchez-Quintana D, Cabrera JA, Climent V, et al. Anatomic relations between the esophagus and left atrium and relevance for ablation of atrial fibrillation. *Circulation* 2005;**112**:1400–5.

53 Cabrera JA, Sánchez-Quintana D, Farré J, et al. Ultrasonic characterization of the pulmonary venous wall. Echographic and histological correlation. *Circulation* 2002;**106**:968–73.

54 Bachmann G. The inter-auricular time interval. *Am J Physiol* 1916;**41**:309–20.

55 Papez JW. Heart musculature of the atria. *Am J Anat* 1920;**27**:255–85.

56 Wittkampf FH, Vonken EJ, Derksen R, et al. Pulmonary vein ostium geometry: analysis by magnetic resonance angiography. *Circulation* 2003;**107**:21–3.

57 Kato R, Lickfett L, Meininger G, et al. Pulmonary vein anatomy in patients undergoing catheter ablation of atrial fibrillation: lessons learned by use of magnetic resonance imaging. *Circulation* 2003;**107**:2004–10.

58 Tsao HM, Yu WC, Cheng HC, et al. Pulmonary vein dilation in patients with atrial fibrillation: detection by magnetic resonance imaging. *J Cardiovasc Electrophysiol* 2001;**12**:809–13.

59 Scharf C, Sneider M, Case I, et al. Anatomy of the pulmonary veins in patients with atrial fibrillation and effects of segmental ostial ablation analysed by computed tomography. *J Cardiovasc Electrophysiol* 2003;**14**:150–5.

60 Lin WS, Prakash VS, Tai CT, et al. Pulmonary vein morphology in patients with paroxysmal atrial fibrillation initiated by ectopic beats originating from the pulmonary veins: implications for catheter ablation. *Circulation* 2000;**101**:1274–81.

61 Mansour M, Refaat M, Heist EK, et al. Three-dimensional anatomy of the left atrium by magnetic resonance angiography: implication for catheter ablation for atrial fibrillation. *J Cardiovasc Electrophysiol* 2006;**17**:719–23.

62 Schmidt B, Ernst S, Ouyang F, et al. External and endoluminal analysis of left atrial anatomy and the pulmonary veins in three-dimensional reconstruction of magnetic resonance angiography: the full insight from inside. *J Cardiovasc Electrophysiol* 2006;**17**:957–64.

63 Wongcharoen W, Tsao HM, Wu MH, et al. Morphologic characteristics of the left atrial appendage, roof, and septum: implication. *J Cardiovasc Electrophysiol* 2006;**17**:951–6.

64 Cosio FG, Anderson RH, Kuck KH, et al. Living anatomy of the atrioventricular junctions: a guide to electrophysiologic mapping. A consensus from the Cardiac Nomenclature Study Group, Working Group of Arrhythmias, European Society of Cardiology, and the Task Force on Cardiac Nomenclature from NASPE. *Circulation* 1999;**100**:e31.

65 Petersen P, Kastrup J, Brinch K, et al. Relation between left atrial dimension and duration of atrial fibrillation. *Am J Cardiol* 1987;**60**:382–4.

66 Yamane T, Shah DC, Jais P, et al. Dilatation as a marker of pulmonary veins initiating atrial fibrillation. *J Interv Cardiac Electrophysiol* 2002;**6**:245–9.

67 Keith A. An account of the structures concerned in the production of the jugular pulse. *J Anat Physiol* 1907;**42**:1–25.

68 Sharma S, Devine W, Anderson RH. The determination of atrial arrangement by examination of appendage morphology in 1842 heart specimens. *Br Heart J* 1988;**60**:227–31.

69 Veinot J, Harrity P, Gentile F, et al. Anatomy of the normal left atrial appendage. A quantitative study of age-related changes in 500 autopsy hearts: implications for echocardiographic examination. *Circulation* 1997;**96**:3112–15.

70 Shadevan J, Ryu K, Peltz L, et al. Epicardial mapping of chronic atrial fibrillation in patients: preliminary observations. *Circulation* 2004;**110**:3293–9.

71 Harada A, Konishi T, Fukata M, et al. Intraoperative map guided operation for atrial fibrillation due to mitral valve disease. *Ann Thoracic Surg* 2000;**69**:446–51.

72 Wu TJ, Doshi RN, Huan HL. Simultaneous biatrial computerized mapping during permanent atrial fibrillation in patients with organic heart disease. *J Cardiovasc Electrophysiol* 2002;**13**:571–7.

73 Marshall J. On the development of the great anterior veins in man and mammalian including an account of certain remnants of foetal structure found in the adult, a comparative view of these great veins in the different mammalian, and an analysis of their occasional

peculiarities in the human subject. *Phil Trans Roy Soc Lond* 1850;**140**:133–69.

74 Sherlag BJ, Yeh BK, Robinson MJ. Inferior interatrial pathway in the dog. *Circ Res* 1972;**31**:18–35.

75 Tai CT, Hsieh MH, Tsai CF, et al. Differentiating the ligament of Marshall from the pulmonary vein musculature potentials in patients with paroxysmal atrial fibrillation: electrophysiological characteristics and results of radiofrequency ablation. *Pacing Clin Electrophysiol* 2000;**23**: 1493–501.

76 Hwang C, Wu TJ, Doshi RN, et al. Vein of Marshall cannulation for the analysis of electrical activity in patients with focal atrial fibrillation. *Circulation* 2000; **101**:1503–5.

77 Lin WS, Tai CT, Hsieh MH, et al. Catheter ablation of paroxysmal atrial fibrillation initiated by non-pulmonary vein ectopy. *Circulation* 2003;**107**:3176–83.

78 Doshi RN, Wu T-J, Yashmina M, et al. Relation between ligament of Marshall and adrenergic atrial tachyarrhythmia. *Circulation* 1999;**100**:876–83.

79 Kurotobi T, Ito H, Inoue K, et al. Marshall vein as arrhythmogenic source in patients with atrial fibrillation: correlation between its anatomy and electrophysiological findings. *J Cardiovasc Electrophysiol* 2006;**17**: 1062–7.

80 Kim DT, Lai AC, Hwang C, et al. The ligament of Marshall: a structural analysis in human hearts with implications for atrial arrythmias. *J Am Coll Cardiol* 2000;**36**:1324–7.

81 Makino M, Inoue S, Matsuyama TA, et al. Diverse myocardial extension and autonomic innervation on ligament of Marshall in humans. *J Cardiovasc Electrophysiol* 2006;**17**:594–9.

82 Roithinger FX, Cheng J, SippensGroenewegen A, Lee RJ, Saxon LA, Scheinman MM, Lesh MD. Use of electroanatomic mapping to delineate transseptal atrial conduction in humans. *Circulation* 1999;**100**:1791–7.

83 Schilling RJ, Kadish AH, Peters NS, Goldberger J, Davies DW. Endocardial mapping of atrial fibrillation in the human right atrium using a non-contact catheter. *Eur Heart J* 2000;**21**:550–64.

84 Villacastin J, Pérez-Castellano N, Moreno J, et al. Left atrial flutter after radiofrequency catheter ablation of focal atrial fibrillation. *J Cardiovasc Electrophysiol* 2003;**14**:417–21.

85 Becker A. Left atrial isthmus: anatomic aspects relevant for linear catheter ablation procedures in humans. *J Cardiovasc Electrophysiol* 2004;**15**:809–12.

86 Wittkampf F, Oosterhout M, Loh P, et al. Where to draw the mitral isthmus line in catheter ablation of atrial fibrillation: histological analysis. *Eur Heart J* 2005;**26**: 689–95.

87 Burch GE, Romey RB. Functional anatomy and "throttle valve" action of the pulmonary veins. *Am Heart J* 1954;**47**:58–66.

88 Nathan H, Eliakim M. The junction between the left atrium and the pulmonary veins. An anatomic study of human hearts. *Circulation* 1966;**34**:412–22.

89 DeAlmeida OA, Bohm GM, De Paulo, et al. The cardiac muscles in pulmonary vein of the rat: a morphological and electrophysiological study. *J Morphol* 1975;**145**: 409–34.

90 Cheung DW. Electrical activity of the pulmonary vein and its interaction with the right atrium in the guinea-pig. *J Physiol* 1981;**314**:445–56.

91 Zipes DP, Knope RF. Electrical properties of the thoracic veins. *Am J Cardiol* 1972;**29**:372–6.

92 Yamane T, Shah DC, Jais P, et al. Electrogram polarity reversal as an additional indicator of breakthroughs from the left atrium to the pulmonary veins. *J Am Coll Cardiol* 2002;**39**:1337–44.

93 Moubarak JB, Rozwadowski JV, Strzalka CT, et al. Pulmonary veins–left atrial junction: anatomic and histological study. *PACE* 2000;**23**:1836–8.

94 Sanchez J, Plumb VJ, Epstein AE, et al. Evidence for longitudinal and transverse fiber conduction in human pulmonary veins. *Circulation* 2003;**108**:590–7.

95 Tritto M, De Ponti R, Zardini M, Spadacini G, Oliveira M, Salerno-Uriarte JA. Electrical connection between pulmonary veins in humans. Evidence after radiofrequency ablation of the venoatrial junction. *Circulation* 2001;**104**:e30–e31.

96 Takahashi A, Iesaka Y, Takahashi Y, et al. Electrical connections between pulmonary veins. Implication for ostial ablation of pulmonary veins in patients with paroxysmal atrial fibrillation. *Circulation* 2002;**105**:2998–3003.

97 Saito T, Waki K, Becker AE. Left atrial myocardial extension onto pulmonary veins in humans: anatomic observations relevant for atrial arrhythmias. *J Cardiovasc Electrophysiol* 2000;**11**:888–94.

98 Spach MS, Barr RC, Jewett PH. Spread of excitation from the atrium into the thoracic veins in human beings and dogs. *Am J Cardiol* 1972;**30**:844–54.

99 Spach MS, Dolber PC. Relating extracellular potentials and their derivatives in anisotropic propagation at a microscopic level in human cardiac muscle. Evidence for electrical uncoupling of side-to-side fiber connection with increasing age. *Circ Res* 1986;**58**:356–71.

100 Hassink RJ, Aretz T, Ruskin J, et al. Morphology of atrial myocardium in human pulmonary veins. A post-mortem analysis in patients with and without atrial fibrillation. J *Am Coll Cardiol* 2003;**42**:108–14.

101 Hocini M, Ho SY, Kawara T, et al. Electrical conduction in canine pulmonary veins. Electrophysiological and anatomical correlation. *Circulation* 2002;**105**:2442–8.

102 Masani F. Node-like cells in the myocardial layer of the pulmonary vein of rats: an ultrastructural study. *J Anat* 1986;**145**:133–42.

103 Pérez-Lugones A, McMahon JT, Ratliff NB, et al. Evidence of specialized conduction cells in human pulmonary veins of patients with atrial fibrillation. *J Cardiovasc Electrophysiol* 2002;**14**:803–9.

104 Morillo CA, Klein GJ, Jones DL, et al. Chronic rapid atrial pacing. Structural, functional and electrophysiological characteristics of a new model of sustained atrial fibrillation. *Circulation* 1995:**91**:1588–95.

105 Jalife J, Berenfeld O, Mansour M. Mother rotors and fibrillatory conduction: a mechanism of atrial fibrillation. *Cardiovasc Res* 2002;**54**:59–70.

106 Mandapati R, Skanes A, Chen J, et al. Stable microreentrant sources as mechanism of atrial fibrillation in the isolated sheep heart. *Circulation* 2000;**101**:194–9.

107 Kalifa J, Tanaka K, Zaitsev A, et al. Mechanism of wave fractionation at boundaries of high-frequency excitation in the posterior left atrium of the isolated sheep heart during atrial fibrillation. *Circulation* 2006;**113**: 626–33.

108 Markides V, Shilling RJ, Ho SY, et al. Characterization of the left atrial activation in the intact human heart. *Circulation* 2003;**107**:733–9.

109 Chauvin M, Shah DC, Haissaguerre M, et al. The anatomic basis of connection between the coronary sinus musculature and the left atrium in humans. *Circulation* 2000;**101**:647–52.

110 Antz M, Otomo K, Arruda M, et al. Electrical conduction between the right atrium and the left atrium via the musculature of the coronary sinus. *Circulation* 1998: **98**:1790–5.

111 Betts TR, Ho SY, Sánchez-Quintana D, et al. Characterization of right atrial activation during coronary sinus pacing. *J Cardiovasc Electrophysiol* 2002;**13**:794–800.

112 Chen SA, Tai CT, Yu WC, et al. Right atrial focal atrial fibrillation: electrophysiologic characteristics and radiofrequency catheter ablation. *J Cardiovasc Electrophysiol* 1999;**10**:328–35.

113 Han J, Good E, Morady F, et al. Esophageal migration during left atrial catheter ablation for atrial fibrillation. *Circulation* 2004;**110**:e528.

114 Lowe MD, Peterson LA, Monahan KH, Asivatham SJ, Packer DL. Electroanatomical mapping to assess phrenic nerve proximity to superior vena cava and pulmonary vein ostia. *Heart* 2004;**90**:24.

115 Sanchez-Quintana D, Cabrera JA, Climent V, et al. How close are the phrenic nerves to cardiac structures? Implications for cardiac interventionalists. *J Cardiovasc Electrophysiol* 2005;**16**:309–13.

116 Bai R, Patel D, di Biase L, et al. Phrenic nerve injury after catheter ablation: should we worry about this complication? *J Cardiovasc Electrophysiol* 2006;**17**:944–8.

117 Tse H-F, Reek S, Timmermans C, et al. Pulmonary vein isolation using transvenous catheter cryoablation for treatment of atrial fibrillation without risk of pulmonary vein stenosis. *J Am Coll Cardiol* 2003;**42**:752–8.

118 Ho SY, Cabrera JA, Sánchez-Quintana D, et al. Vagaries of the vagus nerve: relevance to ablationist. *J Cardiovasc Electrophysiol* 2006;**17**:330–1.

119 Zipes DP, Mihalick MJ, Robbins GT. Effects of selective vagal and stellate ganglion stimulation of atrial refractoriness. *Cardiovasc Res* 1974;**8**:647–55

120 Elvan A, Pride HP, Eble JN, Zipes DP. Radiofrequency catheter ablation of the atria reduces inducibility and duration of atrial fibrillation in dogs. *Circulation* 1995; **81**:2235–44.

121 Liu L, Nattel S. Differing sympathetic and vagal effects on atrial fibrillation in dogs: role of refractoriness heterogeneity. *Am J Physiol* 1997;**273**:H805–H816.

122 Schauerte P, Scherlag BJ, Pitha J, Scherlag MA, Reynolds D, Lazzara R, Jackman WM. Catheter ablation of cardiac autonomic nerves for prevention of vagal atrial fibrillation. *Circulation* 200;**102**:2774–80.

123 Armour JA, Murphy DA, Yuan BX, Macdonald S, Hopkins DA. Gross and microscopic anatomy of the human intrinsic cardiac nervous system. *Anat Rec* 1997;**247**:289–98.

124 Pauza DH, Skripka V, Pauziene N, Stropus R. Morphology, distribution, and variability of the epicardiac neural ganglionated subplexuses in the human heart. *Anat Rec* 2000;**259**:353–82.

125 Chiou CW, Eble JN, Zipes DP. Efferent vagal innervation of the canine atria and sinus and atrioventricular nodes. The third fat pad. *Circulation* 1997;**95**:2573–84.

126 Chevalier P, Tabib A, Meyronnet D, et al. Quantitative study of nerves of the human left atrium. *Heart Rhythm* 2005;**2**: 518–22.

127 Tan AY, Li H, Wachsmann-Hogiu S, Chen LS, Chen PS, Fishbein MC. Autonomic innervation and segmental muscular disconnections at the human pulmonary vein–atrial junction: implications for catheter ablation of atrial–pulmonary vein junction. *J Am Coll Cardiol* 2006;**48**:132–43.